

Assessment of SAPT and Supramolecular EDAs Approaches for the Development of Separable and Polarizable force fields

Sehr Naseem-Khan,[†] Nohad Gresh,[†] Alston J. Misquitta,^{*,‡} and Jean-Philip
Piquemal^{*,†,¶,§}

[†]*Laboratoire de Chimie Théorique, Sorbonne Université, UMR 7616 CNRS, 75005, Paris,
France*

[‡]*School of Physics and Astronomy and the Thomas Young Centre for Theory and
Simulation of Materials at Queen Mary University of London, London E1 4NS, U.K.*

[¶]*Institut Universitaire de France, 75005, Paris, France*

[§]*The University of Texas at Austin, Department of Biomedical Engineering, TX, USA*

E-mail: a.j.misquitta@qmul.ac.uk; jean-philip.piquemal@sorbonne-universite.fr

Abstract

Which is the best reference quantum chemical approach to decipher the energy components of the total interaction energy : Symmetry-Adapted Perturbation Theory (SAPT) or Supermolecular Energy Decomposition Analysis (EDA) methods? With the rise of physically motivated polarizable force fields (polFF) grounded on these procedures, the need to answer such a question becomes critical. We report a systematic and detailed assessment of three variants of SAPT (namely SAPT2, SAPT2+3 and SAPT(DFT)) and three supermolecular EDAs approaches (ALMO, CSOV and RVS). A set of challenging, strongly bound water complexes: $(\text{H}_2\text{O})_2$, $\text{Zn}^{2+} \dots \text{H}_2\text{O}$ and $\text{F}^- \dots \text{H}_2\text{O}$ are used as ‘stress-tests’ for these electronic structure methods. We have developed a procedure to separate the induction energy into the polarization and charge-delocalization using an infinite-order strategy based on SAPT(DFT). This paper aims to provide an overview of the capabilities and limitations, but also similarities, of SAPT and supermolecular EDAs approaches for polFF developments. Our results show that SAPT(DFT)/no S^2 and $\omega\text{B97X-D}||\text{ALMO}$ are the most accurate and reliable techniques.

Introduction

The development of accurate intermolecular potentials is critical for the production of robust and predictive molecular dynamics simulations. These potentials commonly rely on gas phase quantum-chemical data, but sometime can also be combined with condensed phase experimental results as a reference for their parametrization. While emerging techniques such as machine learning tend to fit a large amount of data to provide a black-box prediction of the total intermolecular interaction energy (E_{int}), the development of polarizable force fields (polFF) follows a physics-based strategy. In these approaches, E_{int} is reconstructed upon computing a sum of physically motivated contributions such as: electrostatics, exchange-repulsion, many-body induction including polarization and charge-transfer (charge-

delocalization), and dispersion. Of course, such a strategy requires to go beyond classical force fields definitions and to define more complex functional forms for each component of the interaction potential. However, on a Chemistry point of view, the separable aspect of these potentials (i.e. their ability to reconstruct E_{int} contribution by contribution) brings additional and powerful interpretative capabilities to users as information on the physical origins of the molecular interactions is automatically provided. In our groups, we favour this latter approach.¹⁻⁸ There are now numerous theoretical ways of computing these terms, but there is, as yet, no direct means of experimental validation of all energy components.⁹ Indeed, Experiment essentially captures long-range quantities such as multipole moments and frequency-dependent polarizabilities (See Stone’s book, Ch. 13).¹⁰ Alternatively, one could try to resort to indirect means of assessment to correlate the theoretical predictions to experimental measurements such as bond lengths or spectra^{11,12} but it becomes rapidly tedious when a general force field, i.e. valid for any type of element, has to be derived. For these reasons, the gas phase parametrization of intermolecular potentials remains essentially grounded on theoretical results. It is important to note that such *ab initio* force fields should be transferable enough to be able to conserve their initial parametrization to achieve condensed phase simulations. Therefore, the development of next generation accurate polFF rises the key question of the critical choice of a reference technique able to decipher the physical components of E_{int} . Such an approach should: i) possess an overall accuracy leading to E_{int} values comparable to high level *ab initio* reference data such as CCSD(T); ii) should have a robust numerical stability, satisfactory physical trends and a correct asymptotic behaviour for all its different energetic components. The final challenge here is to also obtain contributions summing up to an accurate and predictive value of E_{int} .

The theoretical methods able to unravel E_{int} energetic components can be separated into two classes of techniques: perturbational and supermolecular. The perturbational approaches compute E_{int} as the sum of physical terms using some form of intermolecular perturbation theory, while the supermolecular strategies decompose a supermolecular inter-

action energy into physical components. Among the perturbational methods, the Symmetry-Adapted Perturbation Theory (SAPT) approach¹³ is the most well-known and widely applied perturbational strategy to compute intermolecular interaction energies between molecular dimers and trimers. Over the years, SAPT has evolved into families of techniques differing one from another based on the choice of the treatment of the intermolecular electronic correlation.^{14–17} These different SAPT methods can now be directly accessed in different codes as SAPT2020 suite of codes,¹⁸ PSI4 package,^{19,20} MOLPRO²¹ and CAMCASP.²² The SAPT2020 code and its earlier versions have been used in pioneering developments in intermolecular potentials for a variety of complexes including high-accuracy potentials for small complexes, or models for water embedding explicit two-body and three-body effects.¹⁸ In parallel, with the development of SAPT(DFT),^{23–28} interaction potentials for small to medium-sized organic molecules have been developed (see for example the reviews by Szalewicz^{29,30} and references therein). Likewise, Misquitta & Stone have pioneered a series of accurate, many-body intermolecular interaction models for small organic molecules with CAMCASP.^{8,31,32} However, both the number and diversity of applications of SAPT increased remarkably following its implementation in the PSI4 package. This was primarily because of the ease of use of PSI4, but also because of the improvements to the computational efficiency of the implementation using techniques like density-fitting. Thus, electrostatic models have been developed based on SAPT within the framework of the AMOEBA³³ and SIBFA³⁴ polFFs in order to include charge penetration effects.³⁵ SAPT has also been used to develop many-body analytical potential functions,^{5,36} and advanced polarizable water models such as AMOEBA+^{7,37} and the Gaussian Electrostatic Model (GEM).^{1,38,39}

On the other hand, supermolecular EDAs for the analysis of the intermolecular interaction energy pre-date the SAPT methods, and continue to be developed. Some of these encompass the Constrained Space Orbital Variation (CSOV),⁴⁰ Reduced Variational Space (RVS),⁴¹ Block Localized Wave Function (BLW)^{42–44} and Absolutely Localized Molecular Orbitals (ALMO)⁴⁵ methods. They decompose E_{int} into Coulomb (electrostatic) and exchange-

repulsion energies at first-order, and polarization and charge-transfer (charge-delocalization) energies at second and higher-orders. RVS and CSOV have been used to demonstrate the importance of the charge-delocalization contribution in water and also in Zn^{2+} complexes.^{46–48} Recently, ALMO was used to refine the AMOEBA model for ion . . . water complexes⁴⁹ and to develop the MB-UCB water model.⁵⁰ Also, supermolecular EDAs have enabled continuous refinements and validations of the SIBFA polarizable force-field.^{2,47,51–54}

In this paper, we seek guidelines for the most robust methods enabling to study strongly polar and ionic complexes which are of critical importance for polFF development. We will assess and compare perturbative and supermolecular approaches on the following complexes (Figure 1) : $(\text{H}_2\text{O})_2$ (neutral), $\text{Zn}^{2+} \dots \text{H}_2\text{O}$ (cationic), $\text{F}^- \dots \text{H}_2\text{O}$ (anionic) and with supporting data for $\text{Cl}^- \dots \text{H}_2\text{O}$ and $\text{OH}^- \dots \text{H}_2\text{O}$ provided in the SI (Figure S1). The choice of Zn^{2+} is motivated by its strong “polarizing” divalent nature, its outstanding role in biochemistry being the second most abundant transition metal in organisms after iron, and as a structural element for Zn-fingers⁵⁵ or as a co-factor.⁵⁶ Due to its key importance in living organisms, H_2O is the first molecule considered for polFF validation. And the ion . . . H_2O interactions are representative of the strongly bound, polar systems found in biological environments. An additional motivation to treat these systems is that they can be considered as ‘stress-tests’ for electronic structure methods owing to the strong polarization and charge-transfer (charge-delocalization) effects at play these complexes. This article is organized as follows: we first describe the SAPT, supermolecular EDAs methods and the polarization model developed in this work. We then assess the accuracy of E_{int} from SAPT models and supermolecular EDAs with respect to CCSD(T), which is the ‘gold standard’ method in quantum chemistry.⁵⁷ This is the first criterion to be validated for the choice of reference for polFF development. We next investigate the effect of the single-exchange, or S^2 , approximation¹³ used to compute higher-order exchange terms in all SAPT methods. Schäffer & Jansen^{58,59} have derived second-order exchange-induction and exchange-dispersion energy terms (at zeroth order in intramolecular correlation) without this approximation. They have

demonstrated the significance of these new terms, particularly the second-order exchange-induction, for strongly bound systems. We finally examine in detail the partitioning of the induction energy into the polarization and charge-delocalization. We demonstrate the numerical advantages of the approach based on regularized SAPT(DFT),⁶⁰ and show how the S^2 approximation has a significant impact on these energies. Also, using polarization models, we estimate the infinite-order polarization and charge-delocalization energies from SAPT(DFT), and compare these to the supermolecular EDAs. We finally put forth a choice of *ab initio* reference for polFF development.

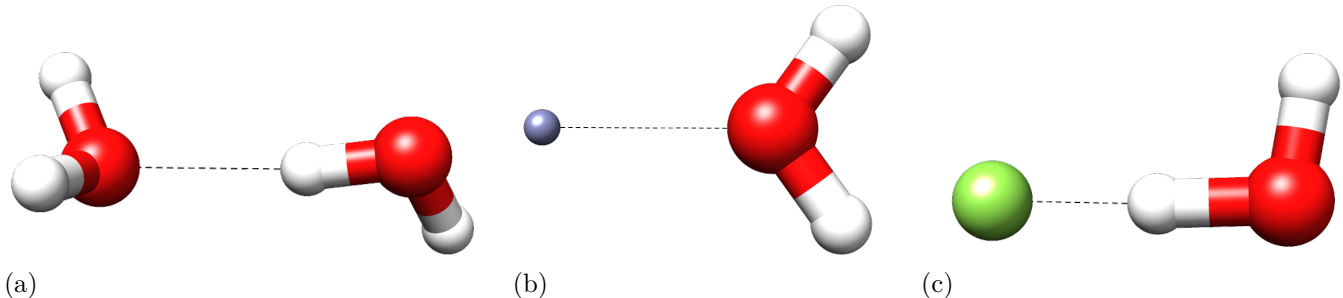


Figure 1: Graphical representation of (a) $\text{H}_2\text{O} \dots \text{H}_2\text{O}$, (b) $\text{Zn}^{2+} \dots \text{H}_2\text{O}$ and (c) $\text{F}^- \dots \text{H}_2\text{O}$ complexes.

Methods

The different supermolecular EDAs and SAPT methods used in this work are first described. Mathematical details can be found in Refs.^{13,23–27,40,41,45} And a definition of charge-transfer (charge-delocalization) and polarization energies within each method is provided as well as a definition of the infinite-order energies from SAPT(DFT).

Charge-delocalization (CD) or charge-transfer (CT)? Note that one of the contributions of the intermolecular interaction energy is associated with the sharing or tunneling of the electrons of the interacting monomers onto the electron-deficient sites of the partners, resulting in a lowering of the energy of the complex. This term is often termed as “charge-transfer” but following Misquitta,^{8,60} we will instead use a more appropriate term i.e.

“charge-delocalization” (CD). While this may seem only a nomenclature issue, as discussed by Misquitta,⁶⁰ and also by Mao *et al.*,⁶¹ the term charge-transfer does not satisfactorily describe the process of electron sharing in a symmetric hydrogen-bonding dimer where there is no net charge transferred from one molecule to the other.

Supermolecular EDAs

Most EDAs resolve the supermolecular interaction energy into five contributions: electrostatic, exchange-repulsion, polarization, charge-delocalization and dispersion, but the decomposition schemes are not unique. A general expression of E_{int} between two monomers A and B can be written as:

$$E_{\text{int}} = E_{\text{elst}} + E_{\text{exch-rep}} + E_{\text{pol}} + E_{\text{cd}} + E_{\text{disp}}. \quad (1)$$

The dispersion contribution is not to be included in the absence of electron correlation. RVS and CSOV decompose E_{int} using similar approaches. Indeed, the variational or the constrained spaces are divided into several sets of orbitals combining occupied and virtual orbitals of monomers A and B. Different constructions of these sets of orbitals allow to compute electrostatic, exchange-repulsion, polarization and charge-delocalization energies. In that case, the charge-delocalization energy is computed as the sum of electron delocalization energies from monomer A towards monomer B, and reciprocally, such as:

$$E_{\text{cd}} = E_{\text{cd}(A \rightarrow B)} + E_{\text{cd}(B \rightarrow A)}. \quad (2)$$

RVS is limited to the Hartree-Fock (HF) level of theory. Thus, computing HF orbitals does not enable to take into account the correlation of opposite spin electrons. CSOV was extended to the DFT level of theory,^{48,62} but can also be used with multi-configurational SCF wavefunctions to access open-shell systems.^{63,64}

On the other hand, the ALMO method decomposes E_{int} at both HF and DFT levels of

theory as:

$$E_{\text{int}}^{\text{ALMO}} = E_{\text{frz}} + E_{\text{pol}} + E_{\text{cd}}, \quad (3)$$

where the E_{frz} term corresponds to the sum of electrostatic and exchange-repulsion energies computed with frozen (frz) orbitals. The ALMO method can be distinguished from RVS and CSOV through the use of absolutely localized molecular orbitals (ALMOs) that are expanded in terms of atomic orbitals (AOs) of a given molecule.⁶⁵ In other words, the ALMOs are centered on the atoms of the monomer as opposed to the MOs in RVS or CSOV which are delocalized over all the monomers. Thus, the use of ALMOs prevents (or suppresses) intermolecular charge delocalization from one monomer to another monomer, allowing then a separation between polarization and charge delocalization terms. The CD-free state interaction energy, $E[\Psi_{\text{ALMO}}]$, is first computed with relaxed ALMOs, and the full interaction energy, $E[\Psi_{\text{full}}]$, is subsequently computed between the fully optimized delocalized MOs, enabling E_{cd} to be derived as:

$$E_{\text{cd}} = E[\Psi_{\text{full}}] - E[\Psi_{\text{ALMO}}]. \quad (4)$$

The RVS, CSOV and ALMO methods all remove the Basis Set Superposition Error (BSSE) within the charge delocalization contribution by using the counterpoise correction.⁶⁶

SAPT methods

Symmetry-Adapted Perturbation Theory (SAPT) is a class of intermolecular perturbation theories which are commonly based on symmetrized Rayleigh–Schrödinger (RS) perturbation theory. It has become common to label SAPT and related methods as EDAs but this may not be appropriate since in SAPT, the interaction energy is built up, term-by-term, to give a total: there is no total energy that is partitioned as is done in supermolecular EDAs. Thus, SAPT based on Hartree–Fock orbitals, or SAPT(HF), is not an EDA for the Hartree–Fock-level interaction energy, even though it can be used to partition $E_{\text{int}}^{\text{HF}}$ if the dispersion term in

SAPT(HF) is neglected. But it is a framework to construct the correlated interaction energy using the Hartree–Fock orbitals as a starting point for the perturbation expansion. Likewise, SAPT(DFT) starts from the Kohn–Sham orbitals and builds up a correlated interaction energy with a possibly further improved accuracy with respect to density-functional theory.

The interaction energy in SAPT can be expressed as a series expansion¹³ as:

$$E_{\text{int}}^{\text{SAPT}} = \sum_{i=1}^{\infty} \sum_{j=0}^{\infty} \left(E_{\text{pol}}^{(ij)} + E_{\text{exch}}^{(ij)} \right), \quad (5)$$

where i and j indicate the order of intermolecular and intramolecular perturbation respectively. The so-called polarization term $E_{\text{pol}}^{(ij)}$ — not to be confused with the polarization energy in a classical polarization model — contains contributions from the electrostatic, induction and dispersion energies. Each of these terms is associated a corresponding exchange term $E_{\text{exch}}^{(ij)}$ that arises from the (anti)-symmetrization procedure. At low orders in the intermolecular perturbation expansion, the SAPT contributions are given specific physical interpretations. For example, we may write the SAPT interaction energy as:

$$\begin{aligned} E_{\text{int}}^{\text{SAPT}} = & \sum_{j=0} \left[E_{\text{elst}}^{(1j)} + E_{\text{exch}}^{(1j)} \right] \\ & + \sum_{j=0} \left[E_{\text{ind,r}}^{(2j)} + E_{\text{ind,exch,r}}^{(2j)} \right] + \delta_{\text{int}}^{\text{HF}}[2] \\ & + \sum_{j=0} \left[E_{\text{disp}}^{(2j)} + E_{\text{disp,exch}}^{(2j)} \right], \end{aligned} \quad (6)$$

where the upper limits of the sums (j) will vary depending on the level of intramolecular correlation included. These terms are commonly regrouped according their physical meaning: electrostatic ($\{E_{\text{elst}}^{(1j)}\}$), exchange-repulsion ($\{E_{\text{exch}}^{(1j)}\}$), induction ($\{E_{\text{ind,r}}^{(2j)}, E_{\text{ind,exch,r}}^{(2j)}\}$) and dispersion ($\{E_{\text{disp}}^{(2j)}, E_{\text{disp,exch}}^{(2j)}\}$). In this illustration, the intermolecular perturbation expansion is conducted only to second-order. Higher-order effects are often important and are approximated using the delta-Hartree–Fock term, $\delta_{\text{int}}^{\text{HF}}[n]$, which approximates polarization and charge-delocalization effects from orders higher than included in the perturbation theory.

Here n is the maximum order of terms included in pure SAPT energies, so $\delta_{\text{int}}^{\text{HF}}[n]$ will include contributions from order $n + 1$ and higher. Since the $\delta_{\text{int}}^{\text{HF}}[n]$ term is non-perturbative, thus it is not strictly a SAPT term. But it often represents a non-negligible contribution to the interaction energy such as strongly hydrogen-bonded complexes. It is commonly included as part of the total induction term. The $\delta_{\text{int}}^{\text{HF}}[2]$ and $\delta_{\text{int}}^{\text{HF}}[3]$ terms, respectively at second and third-order, are computed as:⁶⁷⁻⁶⁹

$$\delta_{\text{int}}^{\text{HF}}[2] = E_{\text{int}}^{\text{HF}} - (E_{\text{elst}}^{(10)} + E_{\text{exch}}^{(10)} + E_{\text{ind,r}}^{(20)} + E_{\text{ind,exch,r}}^{(20)}) \quad (7)$$

and

$$\delta_{\text{int}}^{\text{HF}}[3] = \delta_{\text{int}}^{\text{HF}}[2] - (E_{\text{ind,r}}^{(30)} + E_{\text{ind,exch,r}}^{(30)}). \quad (8)$$

Here $E_{\text{int}}^{\text{HF}}$ is the Hartree–Fock supermolecular interaction energy for the complex. The subscript “r” indicates that the response of interacting orbitals of each dimer is included in the induction terms (orbital relaxation effects).⁷⁰⁻⁷³ Also, depending on the maximum order of the intra and inter-molecular perturbation used, we may define various levels of SAPT: SAPT0, SAPT2, SAPT2+, SAPT2+(3) and SAPT2+3 methods. The terms included in each of the SAPT levels are listed in Table 1.

Table 1: Summary of commonly used SAPT methods.

Electrostatics			Exchange-Repulsion		
SAPT0	$E_{\text{elst}}^{(10)}$		$+E_{\text{exch}}^{(10)}$		
SAPT2	"	$+E_{\text{elst}}^{(12)}$	"	$+E_{\text{exch}}^{(11)}$	$+E_{\text{exch}}^{(12)}$
SAPT2+	"	"	"	"	"
SAPT2+(3)	"	"	"	"	"
SAPT2+3	"	"	"	"	"
Induction					
SAPT0	$+\delta_{\text{int}}^{\text{HF}}[2]$	$+E_{\text{ind},r}^{(20)}$	$+E_{\text{ind},\text{exch},r}^{(20)}$		
SAPT2	"	"	"	$+{}^tE_{\text{ind},r}^{(22)}$	$+{}^tE_{\text{ind},\text{exch},r}^{(22)}$
SAPT2+	"	"	"	"	"
SAPT2+(3)	"	"	"	"	"
SAPT2+3	$+\delta_{\text{int}}^{\text{HF}}[3] - \delta_{\text{int}}^{\text{HF}}[2]$	"	"	"	$+E_{\text{ind},r}^{(30)}$ $+E_{\text{ind},\text{exch},r}^{(30)}$
Dispersion					
SAPT0	$+E_{\text{disp}}^{(20)}$	$+E_{\text{disp},\text{exch}}^{(20)}$			
SAPT2	"	"			
SAPT2+	"	"	$+E_{\text{disp}}^{(21)}$	$E_{\text{disp}}^{(22)}$	
SAPT2+(3)	"	"	"	"	$+E_{\text{disp}}^{(30)}$
SAPT2+3	"	"	"	"	$+E_{\text{disp},\text{exch}}^{(30)}$ $+E_{\text{ind-disp}}^{(30)}$ $+E_{\text{ind-disp},\text{exch}}^{(30)}$

On the other hand, SAPT(DFT) formulates the interaction energy contributions in terms of the density, density-response functions and interaction density matrices, all constructed from Kohn–Sham orbitals and orbital energies, with appropriate response kernels used for the density response functions. The advantage of this approach over the Hartree–Fock-based SAPT is both simplicity and accuracy. The SAPT(DFT) intermolecular interaction energy is the result of a single perturbation theory as the use of Kohn–Sham orbitals mitigates the need for the inclusion of intramolecular correlation effects. Consequently, the SAPT(DFT) interaction energy is written as:

$$\begin{aligned}
E_{\text{int}}^{\text{SAPT(DFT)}} &= E_{\text{elst}}^{(1)} + E_{\text{exch}}^{(1)} \\
&\quad E_{\text{ind}}^{(2)} + E_{\text{ind,exch}}^{(2)} + \delta_{\text{int}}^{\text{HF}}[2] \\
&\quad E_{\text{disp}}^{(2)} + E_{\text{disp,exch}}^{(2)}.
\end{aligned} \tag{9}$$

The numbers in the superscripts correspond to the order of intermolecular perturbation. The second-order energies are computed using coupled Kohn–Sham (CKS) response kernels. However, the one exception is $E_{\text{disp,exch}}^{(2)}$ which in CAMCASP is estimated from the uncoupled-CKS energy $E_{\text{disp,exch}}^{(2)}[\text{UCKS}]$ by scaling as:

$$E_{\text{disp,exch}}^{(2)} \approx E_{\text{disp,exch}}^{(2)}[\text{UCKS}] \times \frac{E_{\text{disp}}^{(2)}}{E_{\text{disp}}^{(2)}[\text{UCKS}]}, \tag{10}$$

where $E_{\text{disp}}^{(2)}[\text{UCKS}]$ is (non-exchange) dispersion energy computed with the uncoupled-CKS kernel. Note that $E_{\text{disp,exch}}^{(2)}$ can also be computed without scaling.⁷⁴

Due to difficulties in deriving the exchange terms of second and higher-orders in the perturbation operator, until very recently, these terms were computed in the S^2 , or single exchange approximation (SEA). This approximation is known to breakdown when the wavefunction overlap of the interacting species increases. In this case, the S^2 approximation results in too little exchange repulsion, and an unphysical overstabilization of the complex.

This has been shown to get worse at higher-orders in perturbation theory.^{58,75} As an empirical approach to partly alleviate the problem,⁷⁶ the higher-order exchange energies can be scaled by the multiplicative factor $p_{\text{ex}}(\alpha)$ as:

$$p_{\text{ex}}(\alpha) = \left(\frac{E_{\text{exch}}^{(10)}}{E_{\text{exch}}^{(10)}(S^2)} \right)^\alpha, \quad (11)$$

where $E_{\text{exch}}^{(10)}(S^2)$ and $E_{\text{exch}}^{(10)}$ are the first-order exchange energies computed with and without the S^2 approximation using the expressions from Jeziorski *et al.*,⁷⁵ and $p_{\text{ex}}(\alpha)$ is a scale factor that can be modulated by the α exponent. The default choice $\alpha = 1$ is used for SAPT calculations as recommended by Parker *et al.*¹⁶

In this work, for the SAPT(DFT) $E_{\text{ind,exch}}^{(2)}$ energy in eq. (9), we have used a formulation of the theory in which the second-order exchange-induction energy is computed without the single-exchange approximation (SAPT(DFT)/no S^2). To do so, we have implemented in the CAMCASP code the spin-summed (closed shell) form of the expression derived by Schaffer & Jansen. This has major consequences for the very strongly bound complexes we have investigated (see §). While the S^2 approximation is still in use in our calculations of the second-order exchange-dispersion energy, this term is usually small enough⁵⁹ that the simple scaling expression²⁷ should be appropriate.

Charge-delocalization energy in SAPT & SAPT(DFT)

In SAPT and SAPT(DFT), the interaction energy is defined as the sum of physically meaningful quantities, however these theories have nothing to say about the charge-delocalization energy. Rather, the charge-delocalization and polarization energies are both part of the induction energy computed from SAPT/SAPT(DFT), and some scheme must be used to separate these. Therefore, Stone and Misquitta (‘SM09’) have proposed a first definition of

the n^{th} order charge-delocalization energy⁷⁷ as:

$$E_{\text{CD}}^{(n)}(\text{SM09}) = E_{\text{IND}}^{(n)}[\text{DC}] - E_{\text{IND}}^{(n)}[\text{MC}], \quad (12)$$

where $E_{\text{IND}}^{(n)}[\text{DC}]$ is the induction energy computed in the dimer centered (DC) basis, while $E_{\text{IND}}^{(n)}[\text{MC}]$ is the energy computed in the monomer centered (MC) basis. Note that $n = 2$ for SAPT0, SAPT2, SAPT2+, and $n = 3$ for SAPT2+(3) and SAPT2+3. The idea here is that the dimer-centered basis allows the description of charge-delocalization-type excitations, while the monomer-centered basis does not. This is the CD definition used in the PSI4 package. But as discussed by Stone & Misquitta, and demonstrated by Misquitta,⁶⁰ this definition has serious deficiencies for large basis sets and short intermolecular separations. In both cases, the monomer-centered basis sets can also describe CD-type excitations, thus leading to ever diminishing allocations of the induction energy to CD upon increasing the basis set.

As an alternative, Misquitta has proposed⁶⁰ a regularization of the electrostatic potential as a means of defining the charge-delocalization. The induction energy is the response of a molecule to the electrostatic potential of the partner (or environment). This potential consists of a well-behaved, repulsive contribution from the electronic density and a singular, attractive contribution from the point nuclear charges. In this viewpoint, charge-delocalization is associated with electron tunneling into the singular nuclear potential, and hence can be suppressed by suitably eliminating the singularity in this potential. This can be done by using a Gaussian screening function to split the $1/r$ nuclear potential into a singular and regularized part⁷⁸ such as:

$$\frac{1}{r} = v_p(r) + v_t(r), \quad (13)$$

where $v_t = \frac{1}{r} (1 - e^{-\eta r^2})$ is the singular, short-ranged part, and $v_p = \frac{1}{r} e^{-\eta r^2}$ the long-ranged, well-behaved part of the nuclear potential. The regularized induction energy is then

computed using the well-behaved, regularized nuclear potential. With a suitable choice of the parameter η , it has been shown that all of the charge-delocalization can be suppressed leading to a ‘pure’ polarization energy. Hence, we may define the charge-delocalization energy at order n as:

$$E_{\text{CD}}^{(n)}(\text{Reg}) = E_{\text{IND}}^{(n)} - E_{\text{IND}}^{(n)}(\text{Reg}). \quad (14)$$

Note that Misquitta has determined that $\eta = 3.0$ a.u. is a suitable choice for a range of molecular systems, though we may expect this parameter to vary with system, albeit to a small extent. The possible dependencies of η upon the nature of the interacting partner(s) will be studied in a separate work.

Polarization models and higher-order charge-delocalization energies within SAPT(DFT)

Presently, using the SM09 method, the charge-delocalization energy from SAPT can be computed at second and third-order only. And if computed using regularized SAPT(DFT), this can be done to second-order only. This poses a problem since there are contributions to induction from higher-order terms, and these can be as important as the second or third-order induction terms. Such higher-order contributions are often estimated using the $\delta_{\text{int}}^{\text{HF}}$ correction. However, as this energy correction is computed in a hybrid approach that combines low-order SAPT0 with supermolecular Hartree–Fock, there is at present no way to decompose the $\delta_{\text{int}}^{\text{HF}}$ term into separate polarization and charge-delocalization. It is actually not clear that such a decomposition is even theoretically feasible, as these effects are sure to couple at higher-orders in perturbation theory. Nevertheless, because of the relative size of the $\delta_{\text{int}}^{\text{HF}}$ correction (it is nearly as large as the second-order induction for the water dimer at equilibrium), the charge-delocalization component of this term must be included if we are not to severely underestimate the charge-delocalization from the SAPT or SAPT(DFT)

approaches.

Recently a method to extract the charge-delocalization component from the $\delta_{\text{int}}^{\text{HF}}$ energy correction was proposed by Misquitta & Stone⁶ and used for the pyridine dimer. In parallel with this work, Gilmore, Stone & Misquitta⁸ have used this method on the water dimer. We describe below the relevant details of the polarization models used in this paper.

The classical polarization energy of an ensemble of molecules (or units) is $E_{\text{pol,cl}} = \sum_A E_{\text{pol,cl}}(A)$, where A is the molecular label. The classical polarization energy of a molecule A is defined as:

$$E_{\text{pol,cl}}(A) = \frac{1}{2} \sum_{a \in A} \sum_{B \neq A} \sum_{b \in B} \sum_{tu} \Delta Q_t^a f_{n(tu)}(\beta_{\text{pol}}^{ab} R_{ab}) T_{tu}^{ab} Q_u^b, \quad (15)$$

where a (b) labels sites in molecule A (B), the ranks of the moments are given in the compact form $t \equiv l\kappa$ where $l = 0, 1, 2, \dots$ is the angular momentum quantum number, and $\kappa = 0, 1c, 1s, \dots, lc, ls$ labels the real components of the spherical harmonics of rank l (see Appendix B in Stone¹⁰). Q_t^a is the multipole moment operator for moment t at site a , and T_{tu}^{ab} is the interaction tensor¹⁰ which describes the interaction between a multipole Q_u^b at site b and a multipole Q_t^a at site a . $f_{n(tu)}(\beta_{\text{pol}}^{ab} R_{ab})$ is a damping function of order n defined below in eq. (17), where β_{pol}^{ab} is the damping parameter for the (ab) site pair, and R_{ab} is the distance between these sites. Here n is a function of the tensor ranks t and u , and if $t = l_1\kappa_1$ and $u = l_2\kappa_2$, then $n = l_1 + l_2 + 1$. Here, we assume that the damping function depends only on the distance R_{ab} between the sites and not on their relative orientation. ΔQ_t^a is the change in multipole moment t at a due to the self-consistent polarization of site a in the field of all sites on *the other* molecules such as:

$$\Delta Q_t^a = - \sum_{a' \in A} \sum_{B \neq A} \sum_{b \in B} \sum_{t'v} \alpha_{tt'}^{aa'} f_{n(t'v)}(\beta_{\text{pol}}^{a'b} R_{a'b}) T_{t'v}^{a'b} (Q_v^b + \Delta Q_v^b), \quad (16)$$

where $\alpha_{tt'}^{aa'}$ is the distributed polarizability for sites (a, a') which describes the response of the multipole moment component Q_t^a at site a to the t' -component of the field at site a' . To

find ΔQ_t^a we need to solve eq. (16) iteratively. If ΔQ_v^b is dropped from the right-hand-side of this equation then the resulting ΔQ_t^a , when inserted in eq. (15) leads to the second-order polarization energy, $E_{\text{pol,cl}}^{(2)}$. In the models constructed here, we have assumed the localized forms of the distributed polarizabilities: $\alpha_{tu}^{aa'} = \alpha_{tu}^a \delta_{aa'}$. The localization is performed using the techniques described by Stone & Misquitta.^{79,80} For the polarization damping we have used the Tang–Toennies⁸¹ damping model:

$$f_n(x) = 1 - e^{-x} \sum_{k=0}^n \frac{x^k}{k!}, \quad (17)$$

where the parameter $x \equiv x_{ab}$ is either related to the site-site separation R_{ab} linearly as $x_{ab} = \beta_{\text{pol}}^{ab} R_{ab}$, or we use the Slater functional form (SlaterFF) relationship:⁸²

$$x_{ab} = \beta_{\text{pol}}^{ab} R_{ab} - \frac{\beta_{\text{pol}}^{ab} R_{ab} (2\beta_{\text{pol}}^{ab} R_{ab} + 3)}{(\beta_{\text{pol}}^{ab} R_{ab})^2 + 3\beta_{\text{pol}}^{ab} R_{ab} + 3}. \quad (18)$$

The SlaterFF relationship has the effect of introducing a separation-dependent damping coefficient and can be beneficial for complexes at very short separations. There could well be other forms for x_{ab} , but these choices were sufficient for the complexes studied in this work.

As we derive the distributed multipoles and distributed anisotropic (localized) polarizabilities using the BS-ISA (Basis-Space Iterated Stockholder Atoms)⁸³ and ISA-Pol⁷⁹ algorithms, the only unknowns in the above definition of the classical polarization energy are the damping parameters. These are determined by fitting the non-iterated classical polarization energy $E_{\text{pol,cl}}^{(2)}$ to a selection of regularized second-order induction energies $E_{\text{IND}}^{(2)}(\text{Reg})$. Subsequently, the infinite-order classical polarization energy, $E_{\text{pol,cl}}^{(2-\infty)}$, is determined by iterating the classical polarization model to convergence. If we approximate the infinite-order induction energy from SAPT(DFT) as:

$$E_{\text{IND}}^{(2-\infty)} \approx E_{\text{IND}}^{(2)} + \delta_{\text{int}}^{\text{HF}}[2], \quad (19)$$

then the infinite-order charge-delocalization energy is defined as:

$$\begin{aligned}
E_{\text{CD}}^{(2-\infty)} &= E_{\text{IND}}^{(2-\infty)} - E_{\text{POL}}^{(2-\infty)} \\
&\approx E_{\text{IND}}^{(2)} + \delta_{\text{int}}^{\text{HF}}[2] - E_{\text{pol,cl}}^{(2-\infty)}.
\end{aligned}
\tag{20}$$

This approach results in a definition of the charge-delocalization energy that is dependent on the polarization model, but from our experience, this dependence is relatively small in practice. From now on, we denote SAPT(DFT)/Pol-Model, the energies obtained using this approach.

Results and Discussion

Accuracy of E_{int}

It is instructive to assess the accuracies of E_{int} from supermolecular EDA and from SAPT methods, in their present stage of development, as compared to CCSD(T) results. The present study focuses on the interactions of strongly bound complexes, in which polarization and/or charge-delocalization are expected to contribute significantly to E_{int} .

Comparison of SAPT, SAPT(DFT) and DFT

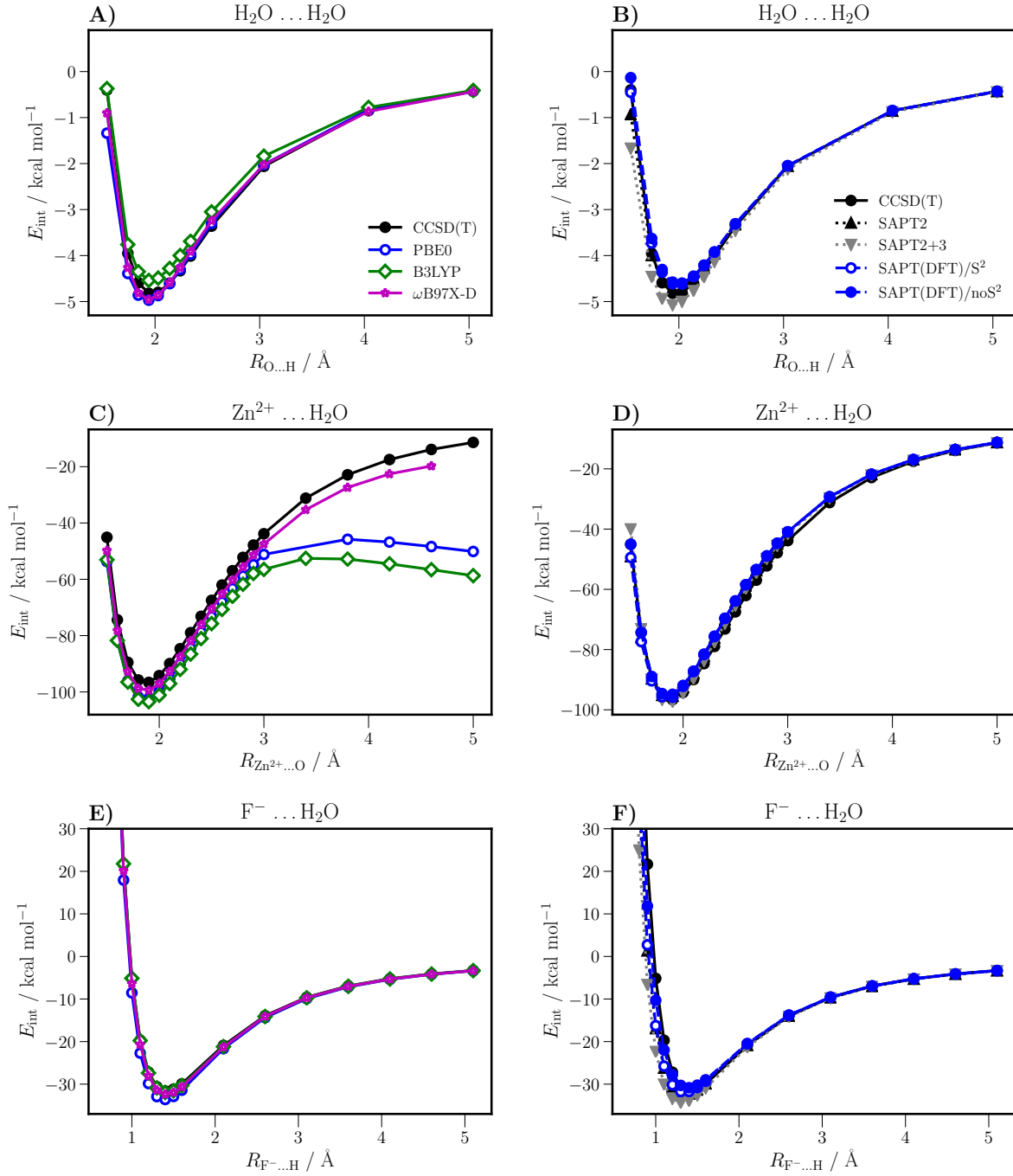


Figure 2: Comparison of the intermolecular interaction energy between DFT-based supermolecular EDAs, SAPT models, SAPT(DFT) and CCSD(T) for the water dimer, Zn²⁺ ... H₂O and F⁻ ... H₂O complexes. The asymptotically corrected PBE0 functional is used for SAPT(DFT). The S^2 approximation is used for the second and third-order exchange energies in the SAPT models and SAPT(DFT)/ S^2 . For SAPT(DFT)/no S^2 this approximation is present only in the $E_{\text{disp,exch}}^{(2)}$ energy.

In Figure 2, we represent the distance evolution of the intermolecular interaction energies of three complexes of a water molecule: with Zn^{2+} , with F^- and with another H_2O molecule. Similar plots for a water molecule with Cl^- and OH^- are in Figure S2 in the SI. It is first observed that the three hybrid functionals, PBE0, $\omega\text{B97X-D}$ and B3LYP, can lead to significant differences in E_{int} . For $(\text{H}_2\text{O})_2$, PBE0 and $\omega\text{B97X-D}$ are nearly identical, even though PBE0 lacks the dispersion correction, and both methods are in good agreement with the CCSD(T) references at longer separations. As the long-range energy of water is dominated by the electrostatic interaction, this is evidence that the densities from these methods are quite accurate. However, B3LYP tends to underestimate the interaction energy at all separations (Fig. 2A). For $\text{F}^- \dots \text{H}_2\text{O}$, all three density functionals give accurate interaction energies. $\omega\text{B97X-D}$ and B3LYP are the most accurate, providing virtually identical interaction energies, while PBE0 overestimates the interaction energy at shorter separations (Fig. 2E). For $\text{Zn}^{2+} \dots \text{H}_2\text{O}$, all functionals overestimate the interaction energy, with $\omega\text{B97X-D}$ showing the smallest errors (around 3%), followed by PBE0 (5%), and B3LYP (7%). At the largest separation, $\omega\text{B97X-D}$ shows closest agreement with CCSD(T), but both PBE0 and B3LYP diverge from CCSD(T) where E_{int} being more negative and a local maximum appears around 3.5 Å. Further convergence was also not possible with all DFT functionals for some geometries at these larger separations (Fig. 2C). An investigation of the charge on the zinc cation shows that the excessive charge delocalization is responsible for these issues. The charge on Zn^{2+} has been computed using an Iterated Stockholder Atoms (ISA) analysis with the CAMCASP code, and AIM (Atom in Molecule) analysis with the GAUSSIAN09 code. We observe that with a Hartree–Fock wavefunction the charge on Zn^{2+} is $+2e$ at long-range, but gets smaller as separation decreases. For example, at 3.0 Å, the charge on Zn^{2+} is $+1.95e$, but with the density functionals this charge is $+1.76e$ (B3LYP), $+1.79e$ (PBE0), and $+1.84e$ ($\omega\text{B97X-D}$). These are all smaller than the charge from HF, with the largest deviations from B3LYP and PBE0. Further, as separation increases, the charge on Zn^{2+} still decreases with the density functionals. For example, by 4.6 Å the zinc charge from $\omega\text{B97X-D}$

decreases to $1.79e$ while the HF charge was already nearly $+2e$ by 3.5 \AA . This means that all density functionals result in an increased, spurious electrostatic interaction between the Zn^{2+} cation and the negatively charged H_2O molecule. This is seen in single-determinant HF and so is not a multi-reference issue, but is more likely related to the delocalization error in DFT. As the $\omega\text{B97X-D}$ functional is a range-separated functional it is more immune to this error, but nevertheless still shows some signs of spurious charge delocalization.

On the other hand, all SAPT methods show high accuracies for all of these systems, including the $\text{Zn}^{2+} \dots \text{H}_2\text{O}$ complex. In all cases, SAPT methods exhibit the correct long-range form, with errors showing up only at very short separations. Indeed, SAPT2+3 shows over-binding compared to SAPT2 for all three complexes (Fig. 2B, D, F). This was not expected as SAPT2+3 includes terms of third order in the intermolecular perturbation operator, but there are theoretical reasons for its lower accuracy (see §). Interaction energies from SAPT(DFT)/no S^2 are in consistently good agreement with the reference CCSD(T) energies. All SAPT(DFT) results were performed using asymptotically corrected PBE0. We have demonstrated in the SI, that contrary to previous statements in the literature⁸⁴ this correction is theoretically needed regardless of the charge state of the interacting species (see Table S1 and Figure S3). The only systematic weakness of SAPT(DFT) and other SAPT methods is the over-binding at very short separations of 1 \AA in the anions $\dots \text{H}_2\text{O}$ interactions (Fig. 2F and S2).

The overall excellent performance of SAPT(DFT) and also SAPT2 make these theories pass the first test of applicability for polFF development. They are consistently accurate for the strongly polar systems of interest, and unlike PBE0, B3LYP and $\omega\text{B97X-D}$, they can be used on all systems (anionic, cationic and neutral) with no strong systematic errors (see also Figure S2 for supporting data on $\text{Cl}^- \dots \text{H}_2\text{O}$ and $\text{OH}^- \dots \text{H}_2\text{O}$ complexes).

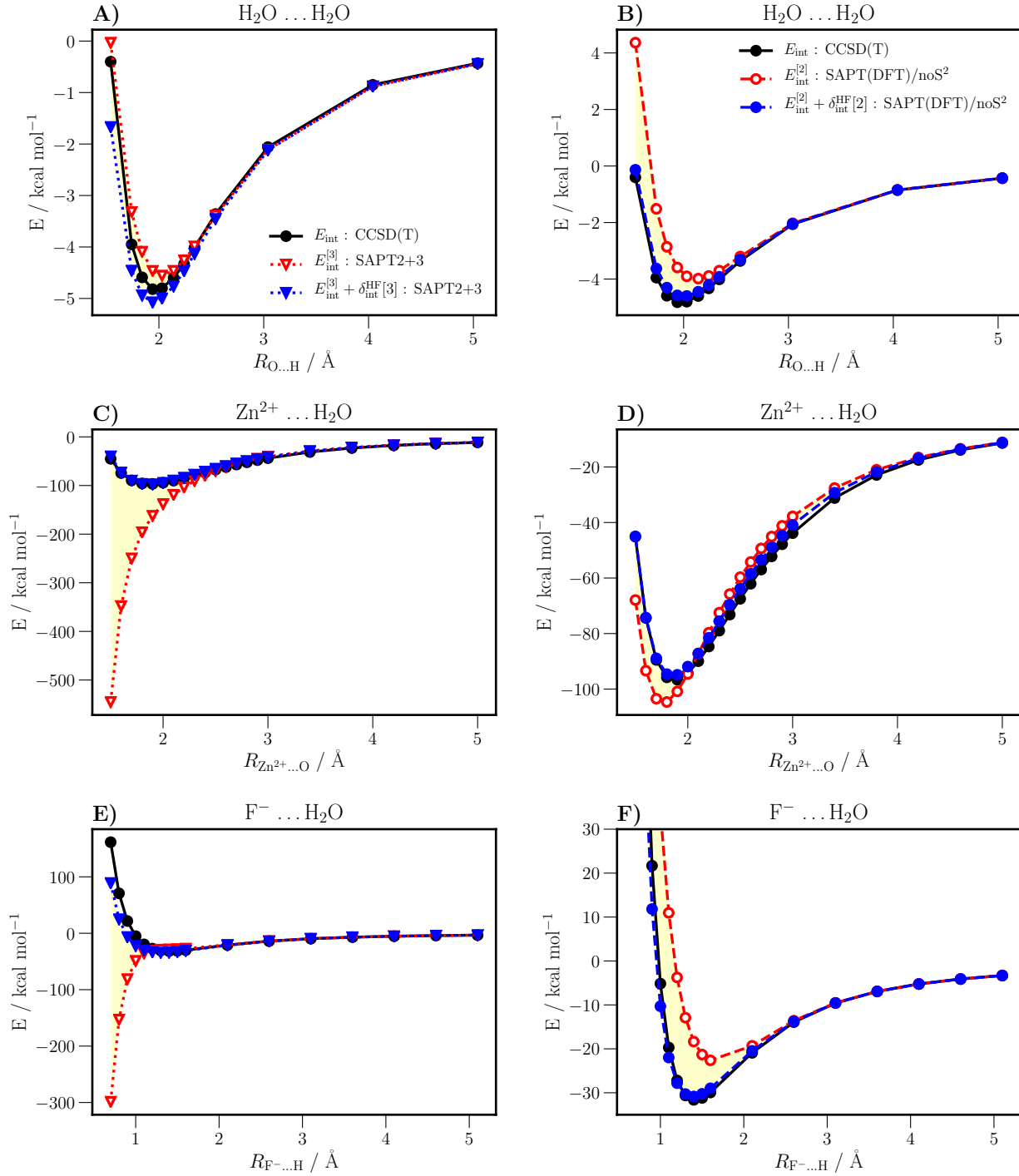


Figure 3: Contribution of the $\delta_{\text{int}}^{\text{HF}}$ energy to the interaction energies from SAPT2+3 and SAPT(DFT). The asymptotically corrected PBE0 functional is used for SAPT(DFT). The S^2 approximation is used for the second and third-order exchange energies in SAPT2+3. For SAPT(DFT) this approximation is present only in the $E_{\text{disp,exch}}^{(2)}$ energy. For SAPT(DFT) the difference between the $E_{\text{int}}^{[2]}$ and $E_{\text{int}}^{[2]} + \delta_{\text{int}}^{\text{HF}}[2]$ curves is the $\delta_{\text{int}}^{\text{HF}}[2]$ contribution, and for SAPT2+3 the difference between the $E_{\text{int}}^{[3]}$ and $E_{\text{int}}^{[3]} + \delta_{\text{int}}^{\text{HF}}[3]$ curves is the $\delta_{\text{int}}^{\text{HF}}[3]$ contribution. These regions are shaded yellow.

Effect of the S^2 approximation on E_{int} and $\delta_{\text{int}}^{\text{HF}}$

In this and subsequent sections we examine the implications of the S^2 approximation on the interaction energies and energy components. As mentioned in § , Schäffer & Jansen have shown that the S^2 approximation causes the second-order exchange energies to be systematically underestimated. And this error gets worse at shorter bond lengths for which orbital overlap effects are larger. The S^2 approximation also has an effect on the $\delta_{\text{int}}^{\text{HF}}[n]$ correction (see eq. (7) and eq. (8)). Figure 3 shows in yellow the difference between $E_{\text{int}}^{[n]}$ (pure SAPT) and $E_{\text{int}}^{[n]} + \delta_{\text{int}}^{\text{HF}}[n]$ for SAPT2+3 and SAPT(DFT) interaction energies. First, we consider the SAPT2+3 results. For $(\text{H}_2\text{O})_2$, $E_{\text{int}}^{[3]}$ is already close to the CCSD(T) references, but upon including $\delta_{\text{int}}^{\text{HF}}[3]$, the total $E_{\text{int}}^{[3]} + \delta_{\text{int}}^{\text{HF}}[3]$, now over-binds, with the location of the minimum and the repulsive wall both moving to shorter O ... H separations (Fig. 3A). For $\text{Zn}^{2+} \dots \text{H}_2\text{O}$ (Fig. 3C) and $\text{F}^- \dots \text{H}_2\text{O}$ (Fig. 3E), the pure SAPT energy $E_{\text{int}}^{[3]}$ shows no minimum, but here the apparent short-range divergence to negative energies is even larger. For neither of these systems does $E_{\text{int}}^{[3]}$ show a minimum. Rather, for $\text{Zn}^{2+} \dots \text{H}_2\text{O}$, $E_{\text{int}}^{[3]}$ appears to diverge, with an energy below $-500 \text{ kcal mol}^{-1}$ at the shortest separation. For $\text{F}^- \dots \text{H}_2\text{O}$, $E_{\text{int}}^{[3]}$ gets close to $-300 \text{ kcal mol}^{-1}$ at the shortest separation. The $\delta_{\text{int}}^{\text{HF}}[3]$ correction, which is predominantly positive for both systems, once again “fixes” the large over-binding of the $E_{\text{int}}^{[3]}$ energies. This results in good agreement with CCSD(T) for $\text{Zn}^{2+} \dots \text{H}_2\text{O}$, but for $\text{F}^- \dots \text{H}_2\text{O}$ $E_{\text{int}}^{[3]} + \delta_{\text{int}}^{\text{HF}}[3]$ from SAPT2+3 still over-binds by around 7% at the minimum and more on the repulsive wall (see the data tables in the SI).

With SAPT(DFT), there is a significantly different outcome. For $(\text{H}_2\text{O})_2$, both $E_{\text{int}}^{[2]}$ and $E_{\text{int}}^{[2]} + \delta_{\text{int}}^{\text{HF}}[2]$ show a minimum, the latter being close to the CCSD(T) reference (Fig. 3B). For $\text{Zn}^{2+} \dots \text{H}_2\text{O}$, in contrast to $E_{\text{int}}^{[3]}$:SAPT2+3 energy, $E_{\text{int}}^{[2]}$:SAPT(DFT) shows a minimum reasonably close to that from CCSD(T) (Fig. 3D), while it over-binds at short separations, this is by less than 10% near the minimum, with no apparent divergence even at the shortest separation of 1.5 \AA . However, upon inclusion of the $\delta_{\text{int}}^{\text{HF}}[2]$ term, the 10% error near the minimum is reduced to less than 2%, and the $E_{\text{int}}^{[2]} + \delta_{\text{int}}^{\text{HF}}[2]$:SAPT(DFT) energies are very

close to the CCSD(T) reference, with the equilibrium distances being nearly identical as well. For $\text{F}^- \dots \text{H}_2\text{O}$, SAPT(DFT) also results in well-behaved interaction energies at the pure SAPT level, $E_{\text{int}}^{[2]}$, and upon inclusion of $\delta_{\text{int}}^{\text{HF}}[2]$, gives $E_{\text{int}}^{[2]} + \delta_{\text{int}}^{\text{HF}}[2]$ energies in very good agreement with CCSD(T) (Fig. 3F). Going further, this analysis has also been conducted at the SAPT2 level for these three complexes. Briefly, we observe a similar behaviour as with SAPT(DFT) for $(\text{H}_2\text{O})_2$ and $\text{F}^- \dots \text{H}_2\text{O}$, but for $\text{Zn}^{2+} \dots \text{H}_2\text{O}$, SAPT2 shows similar problems as made by SAPT2+3 (Figure S4).

Overall, some favorable features are worth noting. Firstly, the consistently good behaviour of SAPT(DFT) for these strongly bound systems is encouraging: the SAPT(DFT) interaction energies are not only reliable as a total, but this total is built from parts themselves well-behaved and thus does not rely on error cancellation. This is the case even at the very short, and nearly chemical bonding separations.

Secondly, the good performance of SAPT(DFT) is to a large extent due to the removal of the S^2 approximation in the major exchange terms. If the S^2 approximation were present in the $E_{\text{ind,exch}}^{(2)}$ and $\delta_{\text{int}}^{\text{HF}}[2]$ energies, SAPT(DFT) would behave like SAPT2. This can be seen from a comparison of Figure S4 and S5 in the SI, where we have displayed SAPT(DFT) energies with the S^2 approximation used in the second-order exchange-induction energies. This is encouraging as it implies that if the S^2 approximation is removed then SAPT2 and also SAPT2+3 could be as well viable alternatives to SAPT(DFT).

In Figures S6 and S7, we have illustrated the extent of the S^2 error in the $E_{\text{IND}}^{(2)}$ energy, and also in the sum $E_{\text{IND}}^{(2)} + \delta_{\text{int}}^{\text{HF}}[2]$. However for all complexes, except at very short separations, the S^2 error is nearly completely cancelled when $\delta_{\text{int}}^{\text{HF}}[2]$ is added to $E_{\text{IND}}^{(2)}$, in agreement with the results of Schäffer & Jansen. Why then do we need bother with the S^2 approximation? The answer is that if we are interested in the individual contributions to the interaction energy, then as demonstrated next, this approximation must be removed.

Separability of the interaction energy

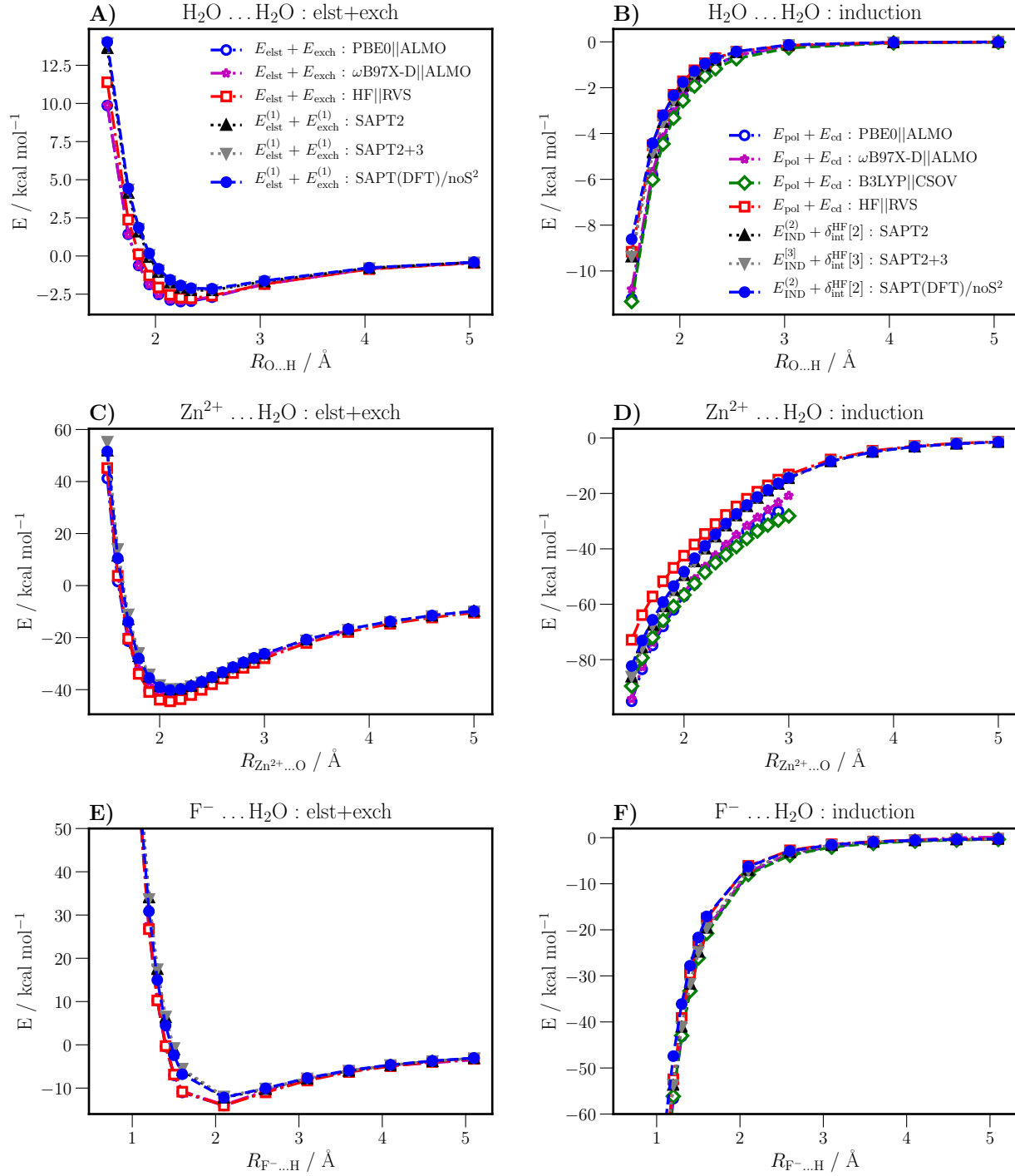


Figure 4: Comparison of the main contributions from SAPT models and SAPT(DFT) with those from supermolecular EDAs for the water dimer, $\text{Zn}^{2+} \dots \text{H}_2\text{O}$ and $\text{F}^- \dots \text{H}_2\text{O}$ complexes. The asymptotically corrected PBE0 functional is used for SAPT(DFT). In the SAPT models, the S^2 approximation is used for the second and third-order exchange energies. For SAPT(DFT) this approximation is present only in the $E_{\text{disp,exch}}^{(2)}$ energy.

The contributions of the interaction energy from SAPT-based methods and supermolecular EDA are compared below. Such comparisons should enable for an informed choice in polFF development to parametrize each separate physical motivated contributions.

Comparison of SAPT, SAPT(DFT) and EDAs

The sum of electrostatic and exchange-repulsion energies, $E_{\text{elst}} + E_{\text{exch}}$, is first analyzed for three of the complexes (Figure 4). We observe that all three SAPT methods give essentially the same energies at all separations, and the supermolecular EDAs are also in mutual agreement. However, there are small but appreciable differences between SAPT and supermolecular EDAs. In the latter, values are always more stabilizing than those from SAPT. For the $(\text{H}_2\text{O})_2$, $\text{Zn}^{2+} \dots \text{H}_2\text{O}$, and $\text{F}^- \dots \text{H}_2\text{O}$ complexes at their equilibrium separations, the difference in $E_{\text{elst}}^{(1)} + E_{\text{exch}}^{(1)}$ from SAPT(DFT) and $E_{\text{elst}} + E_{\text{exch}}$ from $\omega\text{B97X-D||ALMO}$ is slightly larger than 1 kcal mol⁻¹ (Fig. 4A), 3 kcal mol⁻¹ (Fig. 4C), and 5 kcal mol⁻¹ (Fig. 4E), respectively. Such differences of the first-order energies between SAPT and supermolecular EDA methods could be caused by the fact that the latter actually compute the Heitler–London energy. At the HF level, the difference is of the order of S^4 and is almost negligible, but at the DFT level, it is of the order of S^2 and can be large.⁸⁵ Overall, these differences are not negligible when compared with E_{int} , and may well have consequences for the development of polFF with a physical representation of the interaction energy components.

We next consider the total induction energies (Fig. 4B, D, F). For all complexes, the DFT-based supermolecular EDAs give induction energies that are systematically more negative than the SAPT-based ones. PBE0||ALMO and B3LYP||CSOV give nearly the same energies, while $\omega\text{B97X-D||ALMO}$ gives induction energies that are somewhat closer to those from the SAPT methods. This is this likely due to the self-interaction error which results in an over-polarization of the system. As this error is known to decrease with increasing fraction of Hartree–Fock exchange, we should expect the induction energies (in magnitude) to be ordered as follows: B3LYP||CSOV > PBE0||ALMO > $\omega\text{B97X-D||ALMO}$ > SAPT, which is

indeed the case. In the case of $\text{Zn}^{2+} \dots \text{H}_2\text{O}$ (Fig. 4D), the three density functionals EDAs are not only off-set from the SAPT methods as explained above, but appear to diverge from each other. The DFT-based supermolecular EDAs give induction energies that are systematically more negative than the SAPT-based ones by between 7 to 10 kcal mol⁻¹ for the range of $\text{Zn}^{2+} \dots \text{O}$ distances. This difference does not get smaller with increasing separation, but actually *increases* with PBE0||ALMO and B3LYP||CSOV. This effect is unphysical and could pose a significant problem for building polarization models, and we will elaborate on this issue in the next section. In contrast, HF||RVS gives induction energies that are smaller in magnitude than the SAPT values, and these seem to converge to the SAPT energies at long-range. About SAPT-based methods: SAPT2, which has identical total induction with SAPT2+3, and SAPT(DFT) are in overall agreement, with small differences evident only at the shorter intermolecular separations (see also data tables in the SI). This is no doubt due to the cancellation of errors from the S^2 approximation in the pure SAPT energies and the $\delta_{\text{int}}^{\text{HF}}$ terms in SAPT2 and SAPT2+3. In general, SAPT(DFT) gives less negative induction energies than SAPT2, with the largest differences (at equilibrium separations) being 3.9 kcal mol⁻¹ for the $\text{F}^- \dots \text{H}_2\text{O}$ complex (Fig. 4F).

Finally, we examine the trends of the dispersion contribution from the SAPT-based methods. For all three complexes (see Figure S8 in the SI), the $E_{\text{DISP}}^{(2)}$ dispersion energies from SAPT2 and SAPT(DFT) are in good agreement. But the SAPT2+3 $E_{\text{DISP}}^{[3]}$ values are consistently more negative than the $E_{\text{DISP}}^{(2)}$ ones. While this is not surprising, the unusual behaviour of $E_{\text{DISP}}^{[3]}$ for the $\text{Zn}^{2+} \dots \text{H}_2\text{O}$ complex (Fig. S7D) does give us cause for concern. Indeed, $E_{\text{DISP}}^{[3]}$ is substantially more negative than $E_{\text{DISP}}^{(2)}$ from either SAPT2 or SAPT(DFT). But for separations smaller than 1.9 Å it shows a minimum and then gets less negative than $E_{\text{DISP}}^{(2)}$. This is unexpected and likely an unphysical consequence of the S^2 approximation that has a much larger effect on the third-order exchange-dispersion and mixed induction-dispersion exchange energies that are included in $E_{\text{DISP}}^{[3]}$ (see Table 1).

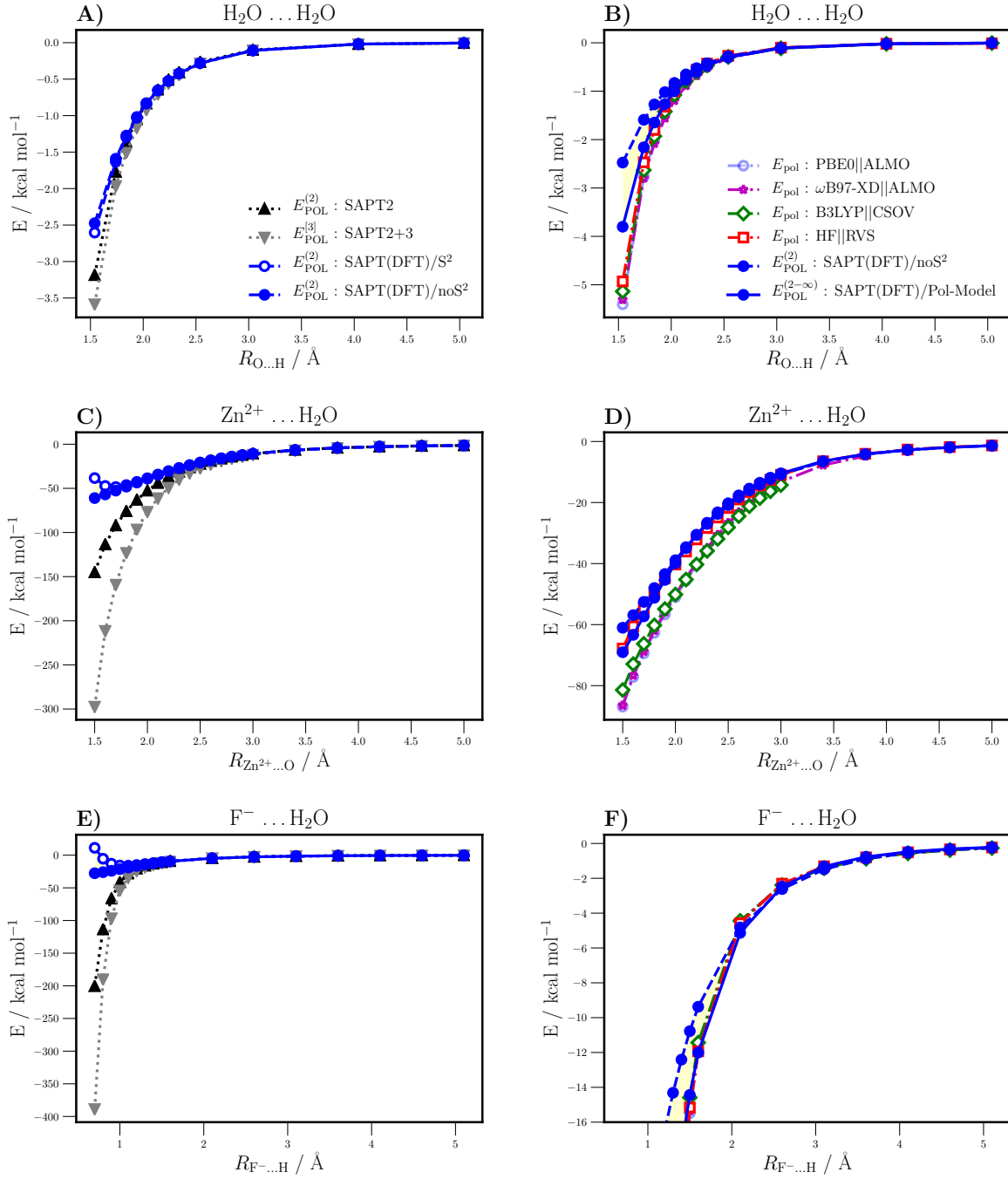


Figure 5: Comparison of E_{POL} from SAPT and the supermolecular EDAs for the water dimer, $\text{Zn}^{2+} \dots \text{H}_2\text{O}$ and $\text{F}^- \dots \text{H}_2\text{O}$ complexes. The S^2 approximation is used for the second and third-order exchange energies in the SAPT models and $\text{SAPT(DFT)}/[\text{PBE0}/\text{AC}/S^2]$. For $\text{SAPT(DFT)}/\text{no}S^2$ this approximation is removed from the energies shown here. And $E_{\text{POL}}^{(2-\infty)} : \text{SAPT(DFT)}/\text{Pol-Model}$ is obtained with the polarization model developed in this work.

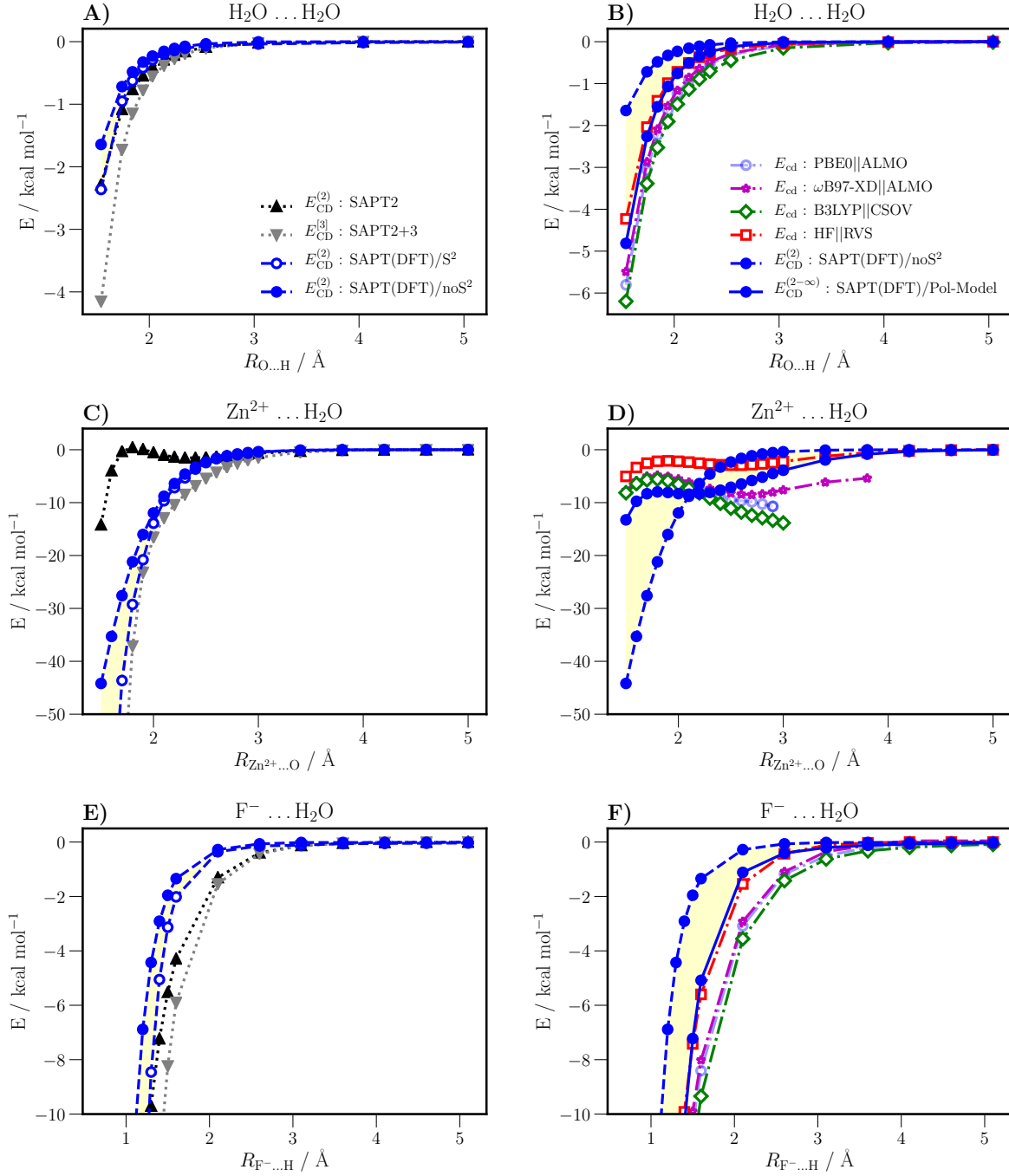


Figure 6: Comparison of E_{CD} from SAPT and the supermolecular EDAs for the water dimer, $Zn^{2+} \dots H_2O$ and $F^- \dots H_2O$ complexes. The S^2 approximation is used for the second and third-order exchange energies in the SAPT models and $\text{SAPT(DFT)}/S^2$. For $\text{SAPT(DFT)}/noS^2$ this approximation is removed from the energies shown here. $E_{CD}^{(2-\infty)}$: $\text{SAPT(DFT)}/\text{Pol-Model}$ is obtained with the polarization model developed in this work. For $F^- \dots H_2O$ calculations with $\omega\text{B97X-D}||\text{ALMO}$ there were numerical issues at the two longest separations and so these have been removed from panel (F) in the figure.

E_{CD} & E_{POL} : variations with methods

In this section, we address the separability of the induction energy into polarization (POL) and charge-delocalization (CD) in the SAPT and supermolecular EDAs methods shown in Figures 5 and 6.

We first compare POL and CD energies obtained with the widely used Stone & Misquitta (SM09) method (SAPT2, SAPT2+3), and the newer regularized charge-delocalization definition (SAPT(DFT)). We observe that the POL and CD energies from SAPT2 and SAPT2+3 are effected by both the S^2 approximation as well as by the use of the SM09 algorithm. As explained above, the S^2 approximation leads to an underestimation of the exchange-induction energies, and consequently increases POL and CD (in magnitude). The SM09 basis-space algorithm for defining the POL and CD energies can be ill-defined when large basis sets are used, or when the complex separation is small. In both cases, it has been shown⁶⁰ that SM09 will lead to more POL and less CD (in magnitude). Therefore, the POL energies from SAPT2 and SAPT2+3 using both the S^2 approximation and SM09 are more negative (Fig. 5A, C, E), but the CD energies are likely less due to a cancellation of errors (Fig. 6A, C, E). On the other hand, in SAPT(DFT), the increased exchange energy present when the S^2 approximation is removed causes $E_{\text{CD}}^{(2)}/\text{no}S^2$ energies to decrease for all systems as expected. But the removal of the S^2 approximation has relatively little effect on $E_{\text{POL}}^{(2)}/\text{no}S^2$ except at the shortest separations for $\text{Zn}^{2+} \dots \text{H}_2\text{O}$ and $\text{F}^- \dots \text{H}_2\text{O}$. In both complexes, $E_{\text{POL}}^{(2)}/\text{no}S^2$ energies are larger in magnitude than $E_{\text{POL}}^{(2)}/S^2$ (Fig. 5C, E). And $E_{\text{POL}}^{(2)}/S^2$ shows an unexpected increase at very short-range (in magnitude) which is not observed in the $E_{\text{POL}}^{(2)}/\text{no}S^2$ energies. We do not as yet understand why this is the case. We suspect that it is an artifact of the regularization potential, which, at these very short separations, is likely to suppress the polarization energy. However, this does not explain why this feature is not present in $E_{\text{POL}}^{(2)}/\text{no}S^2$. Overall, SAPT(DFT)/no S^2 gives consistently physically acceptable estimates for $E_{\text{POL}}^{(2)}$ and $E_{\text{CD}}^{(2)}$ for all three complexes at all intermolecular separations.

Next, since the POL and CD energies from supermolecular EDAs are computed non-

perturbatively, these energies are effectively at infinite-order in the context of intermolecular perturbation. Therefore, when making comparisons with SAPT(DFT), it is essential to ensure that the infinite-order CD and POL energies are used to avoid misleading assessments.^{6,8,60,61} We have done this using the methodology described in § , through which the infinite-order energies are defined with the help of classical polarization models. Details of the construction of these models and their parameters can be found in the SI (Figures S9 and S10). The infinite-order polarization ($E_{\text{POL}}^{(2-\infty)}$) and charge-delocalization ($E_{\text{CD}}^{(2-\infty)}$) energies have then been estimated for SAPT(DFT)/no S^2 . In all systems, the inclusion of higher-order effects in the SAPT(DFT) POL (Fig. 5B, D, F) and CD (Fig. 6B, D, F) energies brings them closer to the corresponding energies from the supermolecular EDAs. Differences nevertheless remain since the SAPT(DFT) POL and CD energies are smaller in magnitude than those from the DFT-based supermolecular EDAs, and often in good agreement with the Hartree–Fock based RVS EDA. For the water dimer, $E_{\text{CD}}^{(2-\infty)}$ from SAPT(DFT) agrees well with the HF||RVS result, but has 0.5 to 1 kcal mol⁻¹ lesser magnitudes than the DFT-based EDA methods at the energetically relevant dimer separations (Fig. 6B). For F⁻...H₂O, there is a much closer agreement between SAPT(DFT) and all supermolecular EDAs regarding E_{POL} (Fig. 5F). However, as with the water dimer, there are large differences (from 2 to 4 kcal mol⁻¹) between the CD energies from SAPT(DFT) and the three DFT-based methods (Fig. 6F). Though these differences are significant, they are much smaller than the differences between the second-order POL and CD energies from SAPT(DFT) and the corresponding energies from the supermolecular EDAs. Therefore, we do see a convergence of these methods, but only when the S^2 approximation is removed, the CD/POL split is defined through the use of regularization, and infinite-order effects are included.

Finally, we discuss the significant variations of POL and CD energies in the SAPT and supermolecular EDA methods seen in the Zn²⁺...H₂O complex. First, we observe a significant overestimation of the polarization energies from SAPT2 and SAPT2+3 when compared to the other methods (Fig. 5C, D). And the CD energies from SAPT2 are close to zero

except at very short separations (Fig. 6C). This arises from the competing S^2 and basis-set effects of the SM09 approach as mentioned above. Second, we see larger differences between SAPT(DFT) and the DFT-based supermolecular EDAs. It was previously observed, for $R_{\text{Zn}^{2+}\dots\text{O}} < 2.5 \text{ \AA}$, that both ALMO and CSOV result in total induction energies about 7 to 10 kcal mol⁻¹ more negative than SAPT (Fig. 4D). This difference originates mainly from the polarization energy which is about 10 kcal mol⁻¹ more negative than with the DFT-based supermolecular EDAs. However, this difference gets smaller upon inclusion of infinite-order effects in SAPT(DFT) (Fig. 5D). Lastly, the $\text{Zn}^{2+}\dots\text{H}_2\text{O}$ complex shows unusual features in the CD energy (Fig. 6D). In the context of SAPT(DFT), $E_{\text{CD}}^{(2)}$ and $E_{\text{CD}}^{(2-\infty)}$ have different radial dependencies, with only $E_{\text{CD}}^{(2)}$ showing a pure exponential decay. Nevertheless, $E_{\text{CD}}^{(2-\infty)}$ does decrease in magnitude with distance while this is not the case for the three DFT-based supermolecular EDAs. The values of CD from B3LYP||CSOV, PBE0||ALMO and $\omega\text{B97X-D||ALMO}$ actually increase in magnitude with distance. This is unphysical and is related to the excessive charge delocalization of the Zn^{2+} cation in the $\text{Zn}^{2+}\dots\text{H}_2\text{O}$ complex in DFT as discussed in § .

The unusual behaviour of the CD energy for $R_{\text{Zn}^{2+}\dots\text{O}} < 2.5 \text{ \AA}$ needs to be commented on: The CD energy from the DFT and HF methods show a non-exponential form, with a maximum just below 2.0 \AA . This feature is more clearly visible in Figure S9 which shows that it is present in the HF energy no matter which EDA is used. As it is present in both HF and DFT, it cannot be because of the well-known self-interaction error in the Kohn–Sham formalism. In fact, this apparently un-physical behaviour of the CD energy was previously observed in early Hartree-Fock RVS studies on complexes of divalent cations with anionic ligands,^{86,87} and more recently for actinide complexes.^{64,88} The present supermolecular EDA interaction energy curves are not the diabatic interaction energy curves that one would expect. It has been shown in many systems involving metal (Mn^{2+} or Mn^{3+}) cations and water that the system ionized to Mn^+ (or Mn^{2+}) and H_2O^+ .^{64,88,89} This effect is observed at the Hartree–Fock level but is prevented in pure SAPT as the formalism enforces closed-

shell systems with fixed charged states. However, it re-enters the SAPT energy through the $\delta_{\text{int}}^{\text{HF}}$ energy, and so the infinite-order CD energies from SAPT(DFT) also display a non-exponential behaviour at short-range. In practice, DFT results tend to exhibit an even larger deviation from exponential decay due to spurious self-interactions.^{90,91}

Overall, SAPT(DFT) estimates for POL and CD energies have in most cases smaller magnitude than either the ALMO or the CSOV ones. Such differences are not sensitive to the choice of functional, whether hybrid or range-separated. But one needs to take into account such issues encountered at short and long-range of separations when developing polFF.

Conclusions and perspectives

We have performed joint SAPT and supermolecular EDAs calculations on a set of strongly bound and challenging complexes: $(\text{H}_2\text{O})_2$, $\text{Zn}^{2+} \dots \text{H}_2\text{O}$ and $\text{F}^- \dots \text{H}_2\text{O}$, with some additional data provided for the $\text{Cl}^- \dots \text{H}_2\text{O}$ and $\text{OH}^- \dots \text{H}_2\text{O}$ complexes. We have unravelled the similarities and differences between these methods in order to define an *ab initio* framework in order to enable the calibration and validation of accurate and separable polarizable force fields. We have paid particular attention to the separation of the induction energy into polarization and charge-delocalization as this is still a contentious issue. In order to address it, we have determined the infinite-order polarization and charge-delocalization energies using SAPT(DFT), Reg-SAPT(DFT) and classical polarization models developed for the three main complexes studied here. We have demonstrated that the use of Reg-SAPT(DFT) is to be preferred over the older basis-space algorithm from Stone & Misquitta,⁷⁷ particularly for strongly bound systems and at short intermolecular separations. Comparisons with the supermolecular EDAs show that the $E_{\text{POL}}^{(2-\infty)}$ and $E_{\text{CD}}^{(2-\infty)}$ energies from SAPT(DFT) are much closer to the ALMO and CSOV ones than are the second-order energies. This is gratifying as these results strongly suggest that there is a convergence of concepts.

Moreover, following the work of Schäffer & Jansen, it is now possible to compute the exchange-induction energy at second-order without the S^2 approximation, and this has been implemented within SAPT(DFT) in the CAMCASP code. This approximation has been known to be invalid at short separations. In this connection, we have observed that the S^2 approximation leads to an unusually strong underestimation of the exchange-induction for the very strongly bound systems we have studied. At third-order, the S^2 approximation can be even more detrimental. At the time this work was conducted, there were no third-order exchange expressions free of the S^2 approximation, however, recently Waldrop and Patkowski have recently derived third-order exchange-induction without this approximation,⁹² consequently it is now possible to compute the most important exchange terms in both SAPT2 and SAPT2+3 without using this approximation. Doing so would put these SAPT methods on par with SAPT(DFT) for strongly bound complexes.

Regarding the supermolecular EDAs: Strong similarities were demonstrated between B3LYP||CSOV, ω B97X-D||ALMO, and PBE0||ALMO. Even with different wavefunctions, these EDAs are in quite good agreement showing similar results for the sum of electrostatic and exchange-repulsion, polarization and charge delocalization. However, there are small, but significant differences between SAPT(DFT) interaction energy components and those from the supermolecular DFT-based EDAs. These differences appear in the sum of the electrostatics and first-order exchange repulsion energies, with all EDAs leading to more negative energies compared with the SAPT(DFT) ones. The total induction energies from these supermolecular EDAs are larger in magnitude compared to SAPT(DFT), the largest differences occurring for the $\text{Zn}^{2+} \dots \text{H}_2\text{O}$ complex. But overall, energies from the EDAs and SAPT(DFT) agree asymptotically, except for the CD energies in $\text{Zn}^{2+} \dots \text{H}_2\text{O}$.

Finally, based on the complexes studies here, our recommended *ab initio* references to develop polFF based on the separability of E_{int} into well-defined physical components are the SAPT(DFT)/no S^2 and ω B97X-D||ALMO methods. Firstly, SAPT(DFT)/no S^2 has been demonstrated to satisfy all requirements, even at the very short intermolecular separations

of 1 Å or less. Contrary to what one might *a priori* suppose, the SAPT formalism does give meaningful and accurate results even at these short separation. Secondly, of the supermolecular EDAs, ω B97X-D||ALMO shows the highest accuracy and the most reliable partitioning. We found this method to be comparable to SAPT(DFT)/no S^2 in accuracy, with interaction energy components from the two techniques in broad agreement, with the exception of the important $\text{Zn}^{2+} \dots \text{H}_2\text{O}$ complex. Lastly, the results of this paper led us to propose some recommendations for SAPT(DFT) calculations in the form of a check-list for force fields developers which are provided in the SI.

Technical Appendix

Numerical details. All calculations have been performed using the aug-cc-pVTZ basis set for the water molecule, the zinc cation and anions (fluoride, chloride and hydroxy). CCSD(T) full electrons calculations were performed with GAUSSIAN09 (D01 version)⁹³ using the counterpoise method to correct the BSSE in the total intermolecular interaction energy. RVS, ALMO and CSOV calculations were performed with the GAMESS(US),⁹⁴ QCHEM⁹⁵ and HONDO^{48,96} softwares, respectively. SAPT2 and SAPT2+3 calculations were performed using the PSI4 package (version 1.1) and SAPT(DFT) with the CAMCASP program (version 6.0). Both SAPT calculations were carried out within the dimer centered basis. SAPT(DFT) calculations were performed using the hybrid ALDA+CHF (Adiabatic Local Density Approximation with coupled Hartree–Fock) kernel with orbitals and orbital energies from the PBE0,^{97,98} and with the Casida–Salahub⁹⁹ asymptotic correction (AC). Previous studies^{23,25,26,100} have shown good results with the PBE0 functional. It was therefore used for SAPT(DFT) calculations. Similarly, the ω B97X-D functional¹⁰¹ was used in ALMO calculations. Basis sets and other numerical settings used for the calculation of distributed multipoles and distributed polarizabilities using the BS-ISA⁸³ and ISA-Pol⁷⁹ algorithms with the CAMCASP code are provided in the SI. Due to limitations of the implementation in

the HONDO code, the B3LYP functional¹⁰² was used for CSOV calculations, while with ALMO we will additionally use PBE0. Comparisons between the two methods will therefore not be completely consistent, but as both use hybrid density functionals, their results may be expected to be comparable. Also, only the polarization and charge-delocalization are reported for CSOV calculations, since RVS and CSOV give the same values for electrostatic and exchange-repulsion.

List of symbol used in this work.

Notation	Definition
E_X	$X =$ <ul style="list-style-type: none"> • elst: electrostatic • exch: exchange-repulsion • pol/POL: polarization (from EDAs/SAPTs) • cd/CD: charge-delocalization (from EDAs/SAPTs) • IND: sum of induction and exchange-induction • DISP: sum of dispersion and exchange-dispersion • inter: total intermolecular interaction
$E_X^{(n)}$	contribution X of order $(n) = 1, 2$ or 3
$E_X^{[n]}$	sum of contribution X of order up to $[n] = 2$ or 3
$\delta_{\text{int}}^{\text{HF}}[n]$	delta Hartree-Fock term of order $n = 2$ or 3
$E_X: F M$	<ul style="list-style-type: none"> • $F = \text{B3LYP, PBE0, } \omega\text{B97X-D}$ • $M = \text{CCSD(T), ALMO, CSOV, RVS}$
$E_X: N$	$N = \text{SAPT2, SAPT2+3, SAPT(DFT)}$
SAPT(DFT)/ S^2	$E_{\text{ind,exch}}^{(2)}$ computed with S^2
SAPT(DFT)/no S^2	$E_{\text{ind,exch}}^{(2)}$ computed without S^2
	$S^2 = \text{Single-Exchange Approximation}$
$E_Y^{(2/3)}: \text{SAPT2/SAPT2+3}$	$Y = \text{POL, CD}$ from the SM09 CD Definition
$E_Y^{(2)}: \text{SAPT(DFT)}$	from the Reg-CD Definition
$E_Y^{(2-\infty)}: \text{SAPT(DFT)/Pol-Model}$	from the polarization model developed in this work

Supporting Information Available

Supporting information contains: (1) Additional data for the $\text{Cl}^- \dots \text{H}_2\text{O}$ and $\text{OH}^- \dots \text{H}_2\text{O}$ complexes, and an analysis of the asymptotic correction for anions, (2) Additional data on the role of the S^2 approximation, (3) Additional data on the separability of the interaction energy, (4) Details of the polarization models used in this paper, (5) Additional figures illustrating the sensitivity of SAPT(DFT) to the choice of wavefunction, (6) A list of recommendations for SAPT(DFT) calculations of the interaction energy, and (7) Energy tables and the complex geometries.

Acknowledgements

This work has received funding from the European Research Council (ERC) under the European Union’s Horizon 2020 research and innovation programme (grant agreement No 810367), project EMC2. AJM and JPP acknowledge funding from RSC (IEC\R2\181027) and CNRS under the joint research project (PRC) grant. Computations have been performed at GENCI on the Occigen machine (CINES, Montpellier, France) on grant no A0070707671. We acknowledge particular thanks to one of our referees for suggesting changes that have considerably increased the scientific content of this paper.

References

- (1) Piquemal, J.-P.; Cisneros, G. A.; Reinhardt, P.; Gresh, N.; Darden, T. A. Towards a force field based on density fitting. *J. Chem. Phys.* **2006**, *124*, 104101.
- (2) Gresh, N.; Cisneros, G. A.; Darden, T. A.; Piquemal, J.-P. Anisotropic, Polarizable Molecular Mechanics Studies of Inter- and Intramolecular Interactions and Ligand-Macromolecule Complexes. A Bottom-Up Strategy. *J. Chem. Theory Comput.* **2007**, *3*, 1960–1986.

- (3) Shi, Y.; Ren, P.; Schnieders, M.; Piquemal, J.-P. *Rev. Comput. Chem. Vol. 28*; John Wiley and Sons, Ltd, 2015; Chapter 2, pp 51–86.
- (4) Jing, Z.; Liu, C.; Cheng, S. Y.; Qi, R.; Walker, B. D.; Piquemal, J.-P.; Ren, P. Polarizable Force Fields for Biomolecular Simulations: Recent Advances and Applications. *Annu. Rev. Biophys* **2019**, *48*, 371–394.
- (5) Melcr, J.; Piquemal, J.-P. Accurate biomolecular simulations account for electronic polarization. *Front. Mol. Biosci.* **2019**, *6*, 143.
- (6) Misquitta, A. J.; Stone, A. J. Ab Initio Atom–Atom Potentials Using CamCASP: Theory and Application to Many-Body Models for the Pyridine Dimer. *J. Chem. Theory Comput.* **2016**, *12*, 4184–4208.
- (7) Liu, C.; Piquemal, J.-P.; Ren, P. AMOEBA+ classical potential for modeling molecular interactions. *J. Chem. Theory Comput.* **2019**, *15*, 4122–4139.
- (8) Gilmore, R. A. J.; Dove, M. T.; Misquitta, A. J. First-Principles Many-Body Non-additive Polarization Energies from Monomer and Dimer Calculations Only: A Case Study on Water. *J. Chem. Theory Comput.* **2020**, *16*, 224–242.
- (9) Andrés, J.; Ayers, P. W.; Boto, R. A.; Carbó-Dorca, R.; Chermette, H.; Cioslowski, J.; Contreras-García, J.; Cooper, D. L.; Frenking, G. t.; Gatti, C. et al. Nine Questions on Energy Decomposition Analysis. *J. Comput. Chem.* **2019**, *40*, 2248–2283.
- (10) Stone, A. J. *The Theory of Intermolecular Forces*, 2nd ed.; Oxford University Press, Oxford, 2013.
- (11) Zhao, L.; von Hopffgarten, M.; Andrada, D. M.; Frenking, G. Energy decomposition analysis. *Wiley Interdiscip. Rev. Comput. Mol. Sci.* **2018**, *8*, e1345.
- (12) Mo, Y. The Resonance Energy of Benzene: A Revisit. *J. Phys. Chem. A* **2009**, *113*, 5163–5169.

- (13) Jeziorski, B.; Moszynski, R.; Szalewicz, K. Perturbation Theory Approach to Intermolecular Potential Energy Surfaces of van der Waals Complexes. *Chem. Rev.* **1994**, *94*, 1887–1930.
- (14) Bukowski, R.; Sadlej, J.; Jeziorski, B.; Jankowski, P.; Szalewicz, K.; Kucharski, S. A.; Williams, H. L.; Rice, B. M. Intermolecular potential of carbon dioxide dimer from symmetry-adapted perturbation theory. *J. Chem. Phys.* **1999**, *110*, 3785–3803.
- (15) Misquitta, A. J.; Bukowski, R.; Szalewicz, K. Spectra of Ar–CO₂ from ab initio potential energy surfaces. *J. Chem. Phys.* **2000**, *112*, 5308–5319.
- (16) Parker, T. M.; Burns, L. A.; Parrish, R. M.; Ryno, A. G.; Sherrill, C. D. Levels of symmetry adapted perturbation theory (SAPT). I. Efficiency and performance for interaction energies. *J. Chem. Phys.* **2014**, *140*.
- (17) Korona, T. *Recent Progress in Coupled Cluster Methods*; Springer, 2010; pp 267–298.
- (18) Garcia, J.; Podeszwa, R.; Szalewicz, K. SAPT codes for calculations of intermolecular interaction energies. *J. Chem. Phys.* **2020**, *152*, 184109.
- (19) Parrish, R. M.; Burns, L. A.; Smith, D. G. A.; Simmonett, A. C.; III, A. E. D.; Hohenstein, E. G.; Bozkaya, U.; Sokolov, A. Y.; Remigio, R. D.; Richard, R. M. et al. Psi4 1.1: An Open-Source Electronic Structure Program Emphasizing Automation, Advanced Libraries, and Interoperability. *J. Chem. Theory Comput.* **2017**, *13*, 3185–3197.
- (20) Turney, J. M.; Simmonett, A. C.; Parrish, R. M.; Hohenstein, E. G.; Evangelista, F. A.; Fermann, J. T.; Mintz, B. J.; Burns, L. A.; Wilke, J. J.; Abrams, M. L. et al. Psi4: an open-source *ab initio* electronic structure program. *Wiley Interdiscip. Rev. Comput. Mol. Sci.* **2012**, *2*, 556–565.

- (21) Werner, H.-J.; Knowles, P. J.; Knizia, G.; Manby, F. R.; Schütz, M. Molpro: a general-purpose quantum chemistry program package. *Wiley Interdiscip. Rev. Comput. Mol. Sci.* **2012**, *2*, 242–253.
- (22) Misquitta, A.; Stone, A. CamCASP: a program for studying intermolecular interactions and for the calculation of molecular properties in distributed form. *University of Cambridge* **2018**,
- (23) Heßelmann, A.; Jansen, G. First-order intermolecular interaction energies from Kohn–Sham orbitals. *Chem. Phys. Lett.* **2002**, *357*, 464–470.
- (24) Heßelmann, A.; Jansen, G. Intermolecular induction and exchange-induction energies from coupled-perturbed Kohn–Sham density functional theory. *Chem. Phys. Lett.* **2002**, *362*, 319–325.
- (25) Heßelmann, A.; Jansen, G. Intermolecular dispersion energies from time-dependent density functional theory. *Chem. Phys. Lett.* **2003**, *367*, 778–784.
- (26) Misquitta, A. J.; Szalewicz, K. Intermolecular forces from asymptotically corrected density functional description of monomers. *Chem. Phys. Lett.* **2002**, *357*, 301–306.
- (27) Misquitta, A. J.; Jeziorski, B.; Szalewicz, K. Dispersion Energy from Density-Functional Theory Description of Monomers. *Phys. Rev. Lett.* **2003**, *91*, 033201.
- (28) Misquitta, A. J.; Podeszwa, R.; Jeziorski, B.; Szalewicz, K. Intermolecular Potentials Based on Symmetry-Adapted Perturbation Theory with Dispersion Energies from Time-Dependent Density-Functional Calculations. *J. Chem. Phys.* **2005**, *123*, 214103.
- (29) Szalewicz, K.; Patkowski, K.; Jeziorski, B. In *Intermolecular Forces and Clusters II*; Wales, D. J., Ed.; Structure and Bonding; Springer: Berlin, Heidelberg, 2005; pp 43–117.

- (30) Szalewicz, K. Symmetry-Adapted Perturbation Theory of Intermolecular Forces. *Wiley Interdiscip. Rev. Comput. Mol. Sci.* **2012**, *2*, 254–272.
- (31) Misquitta, A. J.; Welch, G. W. A.; Stone, A. J.; Price, S. L. A First Principles Prediction of the Crystal Structure of C₆Br₂ClFH₂. *Chem. Phys. Lett* **2008**, *456*, 105–109.
- (32) Misquitta, A. J.; Stone, A. J. Ab Initio Atom–Atom Potentials Using C am CASP: Theory and Application to Many-Body Models for the Pyridine Dimer. *J. Chem. Theory Comput.* **2016**, *12*, 4184–4208.
- (33) Wang, Q.; Rackers, J. A.; He, C.; Qi, R.; Narth, C.; Lagardere, L.; Gresh, N.; Ponder, J. W.; Piquemal, J.-P.; Ren, P. General model for treating short-range electrostatic penetration in a molecular mechanics force field. *J. Chem. Theory Comput.* **2015**, *11*, 2609–2618.
- (34) Narth, C.; Lagardère, L.; Polack, E.; Gresh, N.; Wang, Q.; Bell, D. R.; Rackers, J. A.; Ponder, J. W.; Ren, P. Y.; Piquemal, J.-P. Scalable improvement of SPME multipolar electrostatics in anisotropic polarizable molecular mechanics using a general short-range penetration correction up to quadrupoles. *J. Comput. Chem.* **2016**, *37*, 494–506.
- (35) Piquemal, J.-P.; Gresh, N.; Giessner-Prettre, C. Improved Formulas for the Calculation of the Electrostatic Contribution to the Intermolecular Interaction Energy from Multipolar Expansion of the Electronic Distribution. *J. Phys. Chem. A* **2003**, *107*, 10353–10359.
- (36) Cisneros, G. A.; Wikfeldt, K. T.; Ojamäe, L.; Lu, J.; Xu, Y.; Torabifard, H.; Bartok, A. P.; Csanyi, G.; Molinero, V.; Paesani, F. Modeling molecular interactions in water: From pairwise to many-body potential energy functions. *Chem. Rev.* **2016**, *116*, 7501–7528.
- (37) Liu, C.; Piquemal, J.-P.; Ren, P. Implementation of Geometry-Dependent Charge Flux into the Polarizable AMOEBA+ Potential. *J. Phys. Chem. Lett.* **2020**, *11*, 419–426.

- (38) Duke, R. E.; Starovoytov, O. N.; Piquemal, J.-P.; Andrés, G.; Cisneros, A. GEM*: A Molecular Electronic Density-Based Force Field for Molecular Dynamics Simulations. *J. Chem. Theory Comput.* **2014**, *10*, 1361–1365.
- (39) Piquemal, J.-P.; Cisneros, G. A. In *Many-body effects and electrostatics*; Qiang Cui, P. R., Meuwly, M., Eds.; multi-scale computations of Biomolecules 28; Pan Stanford Publishing, 2016; pp 269–299.
- (40) Bagus, P. S.; Hermann, K.; Bauschlicher, C. W. A new analysis of charge transfer and polarization for ligand-metal bonding: Model studies of Al4CO and Al4NH3. *J. Chem. Phys.* **1984**, *80*, 4378–4386.
- (41) Stevens, W. J.; Fink, W. H. Frozen fragment reduced variational space analysis of hydrogen bonding interactions. Application to the water dimer. *Chem. Phys. Lett.* **1987**, *139*, 15–22.
- (42) Mo, Y.; Gao, J.; Peyerimhoff, S. D. Energy decomposition analysis of intermolecular interactions using a block-localized wave function approach. *J. Chem. Phys.* **2000**, *112*, 5530–5538.
- (43) Mo, Y.; Song, L.; Lin, Y. Block-localized wavefunction (BLW) method at the density functional theory (DFT) level. *J. Phys. Chem. A* **2007**, *111*, 8291–8301.
- (44) Mo, Y.; Bao, P.; Gao, J. Energy decomposition analysis based on a block-localized wavefunction and multistate density functional theory. *Phys. Chem. Chem. Phys.* **2011**, *13*, 6760–6775.
- (45) Khaliullin, R. Z.; Cobar, E. A.; Lochan, R. C.; Bell, A. T.; Head-Gordon, M. Unravelling the origin of intermolecular interactions using absolutely localized molecular orbitals. *J. Phys. Chem. A* **2007**, *111*, 8753–8765.

- (46) Garmer, D. R.; Gresh, N. A comprehensive energy component analysis of the interaction of hard and soft dications with biological ligands. *J. Am. Chem. Soc.* **1994**, *116*, 3556–3567.
- (47) Gresh, N.; Stevens, W. J.; Krauss, M. Mono- and poly-ligated complexes of Zn^{2+} : An ab initio analysis of the metal–ligand interaction energy. *J. Comput. Chem.* **1995**, *16*, 843–855.
- (48) Piquemal, J. P.; Marquez, A.; Parisel, O.; Giessner-Prettre, C. A CSOV study of the difference between HF and DFT intermolecular interaction energy values: The importance of the charge transfer contribution. *J. Comput. Chem.* **2005**, *26*, 1052–1062.
- (49) Mao, Y.; Demerdash, O.; Head-Gordon, M.; Head-Gordon, T. Assessing ion–water interactions in the AMOEBA force field using energy decomposition analysis of electronic structure calculations. *J. Chem. Theory Comput.* **2016**, *12*, 5422–5437.
- (50) Das, A. K.; Urban, L.; Leven, I.; Loipersberger, M.; Aldossary, A.; Head-Gordon, M.; Head-Gordon, T. Development of an Advanced Force Field for Water Using Variational Energy Decomposition Analysis. *J. Chem. Theory Comput.* **2019**, *15*, 5001–5013.
- (51) Gresh, N.; Claverie, P.; Pullman, A. Intermolecular interactions: Elaboration on an additive procedure including an explicit charge-transfer contribution. *Int. J. Chem.* **1986**, *29*, 101–118.
- (52) Piquemal, J.-P.; Gresh, N.; Giessner-Prettre, C. Improved Formulas for the Calculation of the Electrostatic Contribution to the Intermolecular Interaction Energy from Multipolar Expansion of the Electronic Distribution. *J. Phys. Chem. A* **2003**, *107*, 10353–10359.
- (53) Gresh, N.; Piquemal, J. P.; Krauss, M. Representation of Zn(II) complexes in polarizable molecular mechanics. Further refinements of the electrostatic and short-range

- contributions. Comparisons with parallel Ab initio computations. *J. Comput. Chem.* **2005**, *26*, 1113–1130.
- (54) Piquemal, J.-P.; Chevreau, H.; Gresh, N. Toward a Separate Reproduction of the Contributions to the Hartree–Fock and DFT Intermolecular Interaction Energies by Polarizable Molecular Mechanics with the SIBFA Potential. *J. Chem. Theory Comput.* **2007**, *3*, 824–837.
- (55) Maynard, A.; Covell, D. Reactivity of zinc finger cores: analysis of protein packing and electrostatic screening. *J. Am. Chem. Soc.* **2001**, *123*, 1047–1058.
- (56) Lipscomb, W. N.; Sträter, N. Recent advances in zinc enzymology. *Chem. Rev.* **1996**, *96*, 2375–2434.
- (57) Řezáč, J.; Hobza, P. Describing noncovalent interactions beyond the common approximations: How accurate is the "gold standard," CCSD(T) at the complete basis set limit? *J. Chem. Theory Comput.* **2013**, *9*, 2151–2155.
- (58) Schäffer, R.; Jansen, G. Intermolecular exchange-induction energies without overlap expansion. *Theor. Chem. Acc. TCA* **2012**, *131*, 1–10.
- (59) Schäffer, R.; Jansen, G. Single-Determinant-Based Symmetry-Adapted Perturbation Theory without Single-Exchange Approximation. *Mol. Phys.* **2013**, *111*, 2570–2584.
- (60) Misquitta, A. J. Charge-transfer from Regularized Symmetry-Adapted Perturbation Theory. *J. Chem. Theory Comput.* **2013**, *9*, 5313–5326.
- (61) Mao, Y.; Ge, Q.; Horn, P. R.; Head-Gordon, M. On the Computational Characterization of Charge-Transfer Effects in Noncovalently Bound Molecular Complexes. *J. Chem. Theory Comput.* **2018**, *14*, 2401–2417.
- (62) Marquez, A. M.; Lopez, N.; Garcia-Hernandez, M.; Illas, F. Similarities and differences

- in the Hartree–Fock and density-functional description of the chemisorption bond. *Surface Science* **1999**, *442*, 463–476.
- (63) Bauschlicher, C. W.; Bagus, P. S.; Nelin, C. J.; Roos, B. O. The nature of the bonding in XCO for X=Fe, Ni, and Cu. *J. Chem. Phys.* **1986**, *85*, 354–364.
- (64) Marjolin, A.; Gourlaouen, C.; Clavaguéra, C.; Dognon, J.-P.; Piquemal, J.-P. Towards energy decomposition analysis for open and closed shell f-elements mono aqua complexes. *Chem. Phys. Lett.* **2013**, *563*, 25–29.
- (65) Khaliullin, R. Z.; Head-Gordon, M.; Bell, A. T. An efficient self-consistent field method for large systems of weakly interacting components. *J. Chem. Phys.* **2006**, *124*, 204105.
- (66) Boys, S.; Bernardi, F. The calculation of small molecular interactions by the differences of separate total energies. Some procedures with reduced errors. *Molecular Physics* **1970**, *19*, 553–566.
- (67) Jeziorska, M.; Jeziorski, B.; Čížek, J. Direct calculation of the Hartree–Fock interaction energy via exchange–perturbation expansion. The He ... He interaction. *Int. J. Chem.* **1987**, *32*, 149–164.
- (68) Moszynski, R. Symmetry-Adapted Perturbation Theory for the Calculation of Hartree–Fock Interaction Energies. *Mol. Phys.* **1996**, *88*, 741–758.
- (69) Mas, E. M.; Szalewicz, K.; Bukowski, R.; Jeziorski, B. Pair potential for water from symmetry-adapted perturbation theory. *J. Chem. Phys.* **1997**, *107*, 4207–4218.
- (70) Salter, E.; Trucks, G. W.; Fitzgerald, G.; Bartlett, R. J. Theory and application of MBPT (3) gradients: The density approach. *Chem. Phys. Lett.* **1987**, *141*, 61–70.
- (71) Trucks, G. W.; Salter, E.; Sosa, C.; Bartlett, R. J. Theory and implementation of the MBPT density matrix. An application to one-electron properties. *Chem. Phys. Lett.* **1988**, *147*, 359–366.

- (72) Trucks, G.; Salter, E.; Noga, J.; Bartlett, R. Analytic many-body perturbation theory MBPT (4) response properties. *Chem. Phys. Lett.* **1988**, *150*, 37–44.
- (73) Salter, E.; Trucks, G. W.; Bartlett, R. J. Analytic energy derivatives in many-body methods. I. First derivatives. *J. Chem. Phys.* **1989**, *90*, 1752–1766.
- (74) Jansen, G. Symmetry-adapted perturbation theory based on density functional theory for noncovalent interactions. *Wiley Interdiscip. Rev. Comput. Mol. Sci.* **2014**, *4*, 127–144.
- (75) Jeziorski, B.; Bulski, M.; Piela, L. First-order perturbation treatment of the short-range repulsion in a system of many closed-shell atoms or molecules. *Int. J. Quantum Chem.* **1976**, *10*, 281–297.
- (76) Patkowski, K.; Podeszwa, R.; Szalewicz, K. Interactions in diatomic dimers involving closed-shell metals. *J. Phys. Chem. A* **2007**, *111*, 12822–12838.
- (77) Stone, A. J.; Misquitta, A. J. Charge-transfer in Symmetry-Adapted Perturbation Theory. *Chem. Phys. Lett.* **2009**, *473*, 201–205.
- (78) Patkowski, K.; Jeziorski, B.; Szalewicz, K. Symmetry-adapted perturbation theory with regularized Coulomb potential. *J. Mol. Struct. (Theochem)* **2001**, *547*, 293–307.
- (79) Misquitta, A. J.; Stone, A. J. ISA-Pol: Distributed Polarizabilities and Dispersion Models from a Basis-Space Implementation of the Iterated Stockholder Atoms Procedure. *Theor. Chem. Acc.* **2018**, *137*, 153.
- (80) Misquitta, A. J.; Stone, A. J. Accurate induction energies for small organic molecules: I. Theory. *J. Chem. Theory Comput.* **2008**, *4*, 7–18.
- (81) Tang, K. T.; Toennies, J. P. An improved simple model for the van der Waals potential based on universal damping functions for the dispersion coefficients. *J. Chem. Phys.* **1984**, *80*, 3726–3741.

- (82) Van Vleet, M. J.; Misquitta, A. J.; Stone, A. J.; Schmidt, J. R. Beyond Born–Mayer: Improved Models for Short-Range Repulsion in ab Initio Force Fields. *J. Chem. Theory Comput.* **2016**, *12*, 3851–3870.
- (83) Misquitta, A. J.; Stone, A. J.; Fazeli, F. Distributed Multipoles from a Robust Basis-Space Implementation of the Iterated Stockholder Atoms Procedure. *J. Chem. Theory Comput.* **2014**, *10*, 5405–5418.
- (84) Lao, K. U.; Schäffer, R.; Jansen, G.; Herbert, J. M. Accurate Description of Intermolecular Interactions Involving Ions Using Symmetry-Adapted Perturbation Theory. *J. Chem. Theory Comput.* **2015**, *11*, 2473–2486.
- (85) Podeszwa, R.; Pernal, K.; Patkowski, K.; Szalewicz, K. Extension of the Hartree–Fock plus dispersion method by first-order correlation effects. *J. Phys. Chem. Lett.* **2010**, *1*, 550–555.
- (86) Gresh, N. Energetics of Zn²⁺ binding to a series of biologically relevant ligands: A molecular mechanics investigation grounded on ab initio self-consistent field supermolecular computations. *J. Comput. Chem.* **1995**, *16*, 856–882.
- (87) Gresh, N.; Garmer, D. R. Comparative binding energetics of Mg²⁺, Ca²⁺, Zn²⁺, and Cd²⁺ to biologically relevant ligands: combined ab initio SCF supermolecule and molecular mechanics investigation. *J. Comput. Chem.* **1996**, *17*, 1481–1495.
- (88) Gourlaouen, C.; Clavaguéra, C.; Marjolin, A.; Piquemal, J.-P.; Dognon, J.-P. Understanding the structure and electronic properties of Th⁴⁺-water complexes. *Can. J. Chem.* **2013**, *91*, 821–831.
- (89) Corongiu, G.; Clementi, E. Study of the structure of molecular complexes. XVI. Doubly charged cations interacting with water. *J. Chem. Phys.* **1978**, *69*, 4885–4887.

- (90) Mori-Sánchez, P.; Cohen, A. J.; Yang, W. Many-electron self-interaction error in approximate density functionals. *J. Chem. Phys.* **2006**, *125*, 201102.
- (91) Lucas Bao, J.; Gagliardi, L.; Truhlar, D. G. Self-Interaction Error in Density Functional Theory: An Appraisal. *J. Phys. Chem. Lett.* **2018**, *9*, 2353–2358.
- (92) Waldrop, J. M.; Patkowski, K. Nonapproximated third-order exchange induction energy in symmetry-adapted perturbation theory. *J. Chem. Phys.* **2021**, *154*, 024103.
- (93) Frisch, M.; Trucks, G.; Schlegel, H.; Scuseria, G.; Robb, M.; Cheeseman, J.; Scalmani, G.; Barone, V.; Mennucci, B.; Petersson, G. G09 Gaussian Inc. 2009.
- (94) Marquez, A.; Davidson, E. Quantum Chemistry Program Exchange (QCPE). *Indiana University: Bloomington, IN* **1999**, 47405.
- (95) Shao, Y.; Gan, Z.; Epifanovsky, E.; Gilbert, A. T.; Wormit, M.; Kussmann, J.; Lange, A. W.; Behn, A.; Deng, J.; Feng, X. et al. Advances in molecular quantum chemistry contained in the Q-Chem 4 program package. *Mol. Phys.* **2015**, *113*, 184–215.
- (96) Dupuis, M.; Marquez, A.; Davidson, E. HONDO95.3, Quantum Chemistry Program Exchange (QCPE); Bloomington, IN: Indiana University.
- (97) Perdew, J.; Burke, K.; Ernzerhof, M. Phys rev lett 77: 3865. *Errata:(1997) Phys Rev Lett.* **1996**, *78*, 1396.
- (98) Adamo, C.; Barone, V. Toward reliable density functional methods without adjustable parameters: The PBE0 model. *J. Chem. Phys.* **1999**, *110*, 6158–6170.
- (99) Casida, M. E.; Salahub, D. R. Asymptotic correction approach to improving approximate exchange-correlation potentials: Time-dependent density-functional theory calculations of molecular excitation spectra. *J. Chem. Phys.* **2000**, *113*, 8918–8935.

- (100) Misquitta, A. J.; Podeszwa, R.; Jeziorski, B.; Szalewicz, K. Intermolecular potentials based on symmetry-adapted perturbation theory with dispersion energies from time-dependent density-functional calculations. *J. Chem. Phys.* **2005**, *123*, 214103.
- (101) Chai, J.-D.; Head-Gordon, M. Long-range corrected hybrid density functionals with damped atom–atom dispersion corrections. *Phys. Chem. Chem. Phys.* **2008**, *10*, 6615–6620.
- (102) Stephens, P.; Devlin, F.; Chabalowski, C.; Frisch, M. J. Ab initio calculation of vibrational absorption and circular dichroism spectra using density functional force fields. *J. Phys. Chem.* **1994**, *98*, 11623–11627.

Graphical TOC Entry

